Transportation Research Part C 159 (2024) 104469

Contents lists available at ScienceDirect

Transportation Research Part C

journal homepage: www.elsevier.com/locate/trc

Planning dynamic wireless charging infrastructure for battery electric bus systems with the joint optimization of charging scheduling

Wenlong Li [a], Yi He [b], Songhua Hu [c], Zhengbing He [c,*], Carlo Ratti [c]

[a] Beijing Key Laboratory of Traffic Engineering, Beijing University of Technology, China
[b] National Renewable Energy Laboratory, United States
[c] Senseable City Lab, Massachusetts Institute of Technology, United States

ARTICLE INFO

Keywords:
Infrastructure planning
Charging scheduling
Integrated optimization
Dynamic wireless charging
Battery electric bus

ABSTRACT

To address the battery-related shortcomings of battery electric buses (BEBs), dynamic wireless charging (DWC) technology that allows BEBs to charge while in motion has emerged, thereby extending the driving range and reducing the size of onboard batteries. The introduction of DWC technology raises a critical problem, namely, the deployment of DWC facilities. To resolve the infrastructure planning problem, this study first proposes a (higher-level) strategic planning model that optimizes the deployment of DWC facilities and battery capacity of BEBs, and then establishes a (lower-level) tactical planning model of optimal charging scheduling under the time-of-use (TOU) tariff mechanism considering the interdependence between infrastructure design and charging activities of BEBs. Mixed-integer nonlinear programming (MINLP) is proposed to optimize the model, aiming to minimize the overall cost associated with charging facilities, batteries, and charging. The proposed optimization model is tested and evaluated using a real-world bus system network, and the results demonstrate that the model effectively determines the DWC facility locations and battery sizes and optimizes the charging scheduling considering the TOU tariff for BEBs. The proposed model in this study provides a comprehensive guideline for relevant practitioners and further promotes the application of DWC technology in BEBs.

1. Introduction

1.1. Background

According to the International Energy Agency, the transportation sector has the highest dependency on fossil fuels among all industries, accounting for 37% of total carbon dioxide emissions in 2021 (IEA, 2021). In some countries, such as China, the total emissions of pollutants from automotive exhaust reached 15.577 million tons in 2021 (MEE, 2021). The pollution generated by combustion engine vehicles has already caused significant harm to the environment. To address the climate crisis and alleviate energy shortages, the electrification of urban bus systems arises as an effective policy option in the field of public transportation. Especially, battery electric buses (BEBs) are garnering growing attention because of their merits such as cleanliness and high efficiency. Currently, many countries and companies are actively developing the BEBs technology, such as Bombardier (Cirimele

* Corresponding author.
E-mail address: he.zb@hotmail.com (Z. He).

https://doi.org/10.1016/j.trc.2023.104469
Received 2 August 2023; Received in revised form 27 November 2023; Accepted 26 December 2023

et al., 2018), the United States (Fuller, 2016), South Korea (Hwang et al., 2018). It is evident that the use of BEBs in urban public transportation has become a mainstream trend. However, some battery-related weaknesses, such as limited range, lengthy charging time, and high battery costs, largely arrest the practical development and applications of BEBs.

The emergence of dynamic wireless charging (DWC) technology, which is considered a promising improvement direction for the BEB system in the future, is expected to resolve these problems (Tan et al., 2022). The concept of DWC was initially proposed in the 1970s (Bolger et al., 1978) and has experienced rapid development over the past decade. Unlike fixed charging facilities, DWC facilities allow BEBs to charge in motion, thereby extending the service range of BEBs (Jansuwan et al., 2021) and saving more energy (Bi et al., 2019). Furthermore, DWC technology allows BEBs to operate with smaller battery capacities and reduces battery costs. Nevertheless, the deployment of the charging facility and the optimal battery capacity are significant variables, which are interdependent and have a direct impact on the charging scheduling of BEBs. Similarly, charging scheduling for BEBs also impacts the infrastructure planning (Liu et al., 2021). Therefore, jointly optimizing the deployment of DWC facilities, the battery capacity of BEBs, and the charging schedule considering the time-of-use (TOU) tariff is crucial for applying the DWC technology in the BEB system.

1.2. Literature review

The optimization problems of a BEB system can be generally divided into three categories: (1) strategic planning problems that mainly involve long-term optimization of a BEB system, (2) tactical planning problems that mainly consider short-term management issues in a BEB system, and (3) operational planning problems that primarily focus on optimizing the real-time operation of buses within a BEB system (Perumal et al., 2022).

The strategic planning problems primarily concentrate on the infrastructure planning for a BEB system. For example, Xylia et al. (2017) employed relevant geographic and urban data to calibrate parameters associated with BEBs and select optimal charging stations from a series of alternative sites in a bus network. Zhang et al. (2022) considered various charging methods and their impact on the degradation of battery capacity and proposed a bi-level programming model to address the location of charging stations. An (2020) proposed a stochastic integer program to optimize the deployment of charging infrastructures and fleet size of BEBs, considering the charging demand uncertainty. Lin et al. (2019) proposed a multiple stages planning model that optimizes the deployment of charging stations, considering the connectivity of power grids and transportation networks.

Regarding the tactical planning problems, some studies mainly focus on optimizing the charging scheduling for BEBs to minimize overall charging costs. For instance, Abdelwahed et al. (2020) introduced two optimization approaches that focus on charging time and charging events, respectively. These approaches aim to optimize the charging schedules for BEBs by utilizing real bus operation data. Tang et al. (2019) proposed a robust optimization model based on real-time traffic conditions to dynamically adjust the charging strategy for BEBs. Additionally, a few studies further optimized the charging timetable of BEBs by considering the TOU tariff. For example, He et al. (2022b) developed a general model for optimizing the charging strategy of BEB systems under the TOU mechanism. Liu et al. (2022) considered the uncertainty of energy consumption and further proposed a robust optimization model to optimize the charging scheduling of BEBs.

For operational planning problems, existing studies mainly concentrate on the scheduling of BEBs and drivers. Boyer et al. (2018) optimized the drivers scheduling under constraints of limited continuous working time and total working hours by proposing a model and solving it using neighborhood search methods. Xie et al. (2023) proposed a coordinated optimization model for bus timetables and driver scheduling by considering different charging modes for BEBs.

Additionally, several studies have integrated these three levels of optimization problems to conduct comprehensive research. Wang et al. (2023) and He et al. (2022a) introduced integrated optimization frameworks that combine the deployment of fixed charging stations and charging scheduling for BEBs. To minimize the total cost of the BEB system, Rogge et al. (2018) proposed a mixed-integer linear programming (MILP) model to optimize charging station locations, fleet sizes on each route, and departures timetable. Focusing on the bus scheduling problem, Liu and Ceder (2020) proposed a multi-objective optimization model to minimize the bus procurement cost and the number of required charging facilities.

It is commonly assumed in the aforementioned literature that BEBs mainly utilize the plug-in charging method. The emergence of DWC technology has completely changed the previous charging approach. As a result, optimization methods proposed in previous studies may not be applicable to DWC facilities.

The deployment of charging facilities poses a critical challenge in the practical implementation of DWC technology. It impacts the maximum energy that BEBs can obtain in the BEB system. To ensure the normal operation of BEBs and minimize the overall cost of the system, it is required further optimization for the battery capacity and charging scheduling. Therefore, the flexibility provided by DWC technology requires special consideration for optimizing the deployment of charging facilities for the BEB system. Some relevant studies have been conducted on the deployment problem of DWC facilities, particularly from the perspectives of traffic network flow allocation and system management.

From the perspective of traffic network flow allocation, Chen et al. (2016) considered the traffic flow distribution in a user equilibrium mode and optimized the deployment of charging lanes in the road network. He et al. (2020b) further examined the negative effects of charging lane placement on road capacity and enhanced the optimization deployment of charging lanes. Ngo et al. (2020) considered the influence of DWC facilities on traffic flow allocation and constructed a model to optimize the location of DWC facilities in the road network.

From the perspective of system management and decision-making, Jeong et al. (2015) considered the economics of DWC facilities within the BEB system, and formulated an economic model to determine the optimal deployment of DWC facilities on routes, by

minimizing the total cost of charging facilities and batteries. Liu and Song (2017) and Bai et al. (2022) further considered the optimal location of charging facilities in a more complex system composed of multiple routes, and incorporated the energy consumption uncertainty during the operation of BEBs, thus transforming the proposed deterministic model into robust optimization models. Additionally, the optimization of dynamic wireless charging systems for BEBs was also investigated by incorporating multiple levels of problems. Alwesabi et al. (2021) integrated the optimization of charging facility deployment, battery capacity, and bus scheduling on each bus route. Furthermore, Alwesabi et al. (2022) further considered the uncertainty during the operation of BEBs and proposed a corresponding robust optimization model.

1.3. Contributions

Despite the increasing research on optimization problems in BEB systems, the existing research efforts have mostly been limited to optimizing the BEB system from a single level. More specifically, the research on the strategic planning problems usually assumes or completely ignores charging scheduling strategies, while focusing on the infrastructure planning. Conversely, the research on the tactical planning problems focuses on optimizing the charging scheduling of BEBs, assuming that charging facility locations and battery sizes are known in advance. These studies do not consider the interrelation between infrastructure planning and charging scheduling, which is critical considering the fact: the deployment of DWC facilities determines the occurrence of charging activities; the charging scheduling alters the battery state of charge (SOC) during the operation of BEBs, thus influencing the battery capacity and the deployment number (length) of charging facilities. In addition, insufficient attention has been devoted to assessing the influence of electricity pricing policies on charging scheduling. The presence of the TOU tariff results in excessive charging costs and affects the charging scheduling of BEBs.

To fill these gaps, this study jointly addresses two optimization problems: the long-term strategic optimization problem and the short-term tactical optimization problem. The former aims to minimize the overall cost by optimizing the deployment of the DWC facility and battery capacity for BEBs. The latter aims to minimize charging costs by optimizing the charging scheduling for BEBs within the BEB system throughout the day. A series of numerical studies conducted in Beijing demonstrates the model's effectiveness in reducing the overall cost. The study provides significant foresight and reference for the application of DWC technology and the electrification transformation of BEB systems. In summary, the primary contributions of this study are as follows.

- An MINLP model is proposed to address the deployment of DWC facilities, battery capacity, and charging scheduling problems in urban BEB systems. With the aim of cost minimization, this study ultimately determines the optimal locations for DWC facilities, battery sizes for BEBs, and charging scheduling strategies based on real-time TOU tariff mechanisms.
- The proposed MINLP model is linearized into an MILP model, making it possible to resolve the reformulated model using widely existing solvers.
- The proposed model that considers the charging scheduling of BEBs turns out a 10.12% reduction in total costs, compared to the existing methods. A series of sensitivity analyses were performed on key parameters of the model, demonstrating the efficiency of the proposed model in minimizing the total cost through a balanced consideration of DWC facility, battery, and charging costs when parameters vary.

1.4. Organization

The remainder of this study is organized as follows. Sections 2 and 3 present the problem description and define a feasible region for a strategic planning problem to optimize the infrastructure planning, respectively. Section 4 proposes a tactical planning program to refine the charging scheduling of BEBs by taking the TOU tariff into account. Section 5 develops an integrated planning model to determine the optimal deployment of the facility, battery capacity, and charging scheduling by minimizing the total cost. Section 6 demonstrates the proposed model in real-world data-based numerical experiments. Section 7 concludes this study.

2. Problem description

A BEB system consists of BEBs, bus routes, depots, terminals, stops, and charging facilities. The terminal connected to the depot is defined as the base station, which is important to gather and distribute the BEBs in the system. Each bus route has one or more terminals.

Fig. 1 provides an illustration of the BEB system, which can be classified into three route types. Route type 1 (cyan line) is the route between bus terminals (base station) and the depot. BEBs leave and return to the depot when they start and finish the service for one day. Route type 2 (purple line) represents the route between terminals. Route type 3 (red line) is a unique circular route type where the start and end terminals of BEBs are identical (Terminal 1). To present the process of BEBs operation in the BEB system with DWC facilities, an illustration is drawn as shown in Fig. 2(a), which uses Route type 1 and 3 as an example.

At the start of service trips, BEBs are fully charged at the depot. While BEBs are in service, they can utilize the available DWC facilities buried under the road to charge their batteries. Upon completing a trip, BEBs idle in the base station until their next journey, utilizing the charging facilities at the base station to recharge their batteries during this period. After completing their service trips for the day, BEBs return directly to the depot and utilize the nighttime for recharging. As shown in Fig. 2(b), the DWC facility consists of an inverter and wireless power transfer coils. The inverter is installed at the start of the DWC facility to transfer electric power to coils, which are employed in a series track and connected to the inverter.

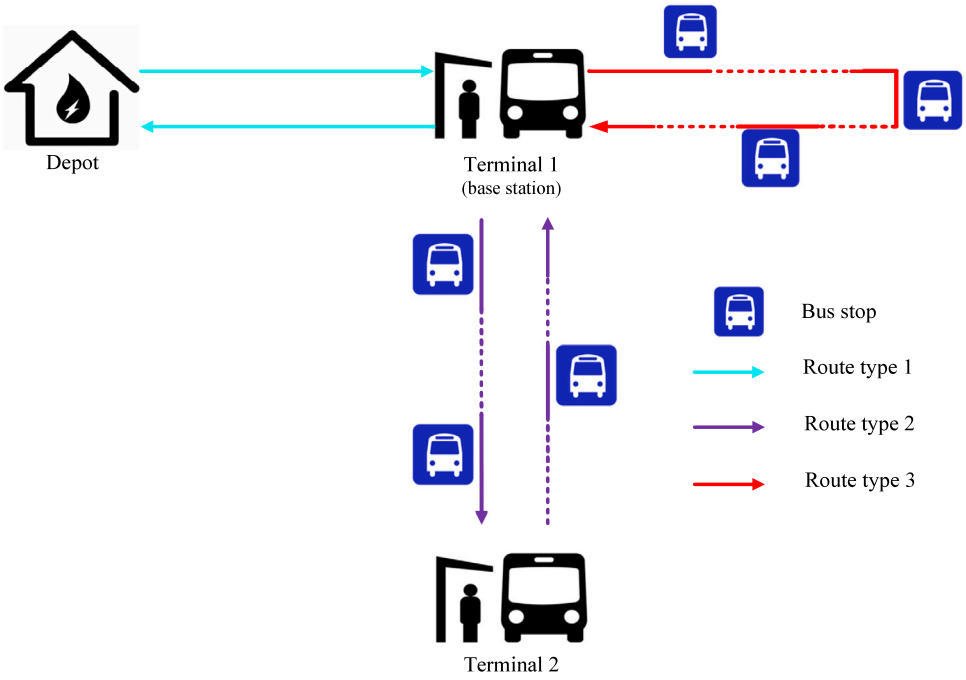

Fig. 1. An illustration of the BEB system.

Traditional BEBs can replenish battery energy by utilizing plug-in chargers installed at the depot and terminals. However, this charging method imposes restrictions on BEBs, which can only be recharged when idle in terminals or depots. It results in a limited available charging time for BEBs, requiring them to carry larger batteries. Conversely, The DWC facility offers more flexibility than plug-in chargers. It can be installed at any location along the routes and allows BEBs to recharge while in motion. Therefore, DWC facilities can provide more charging opportunities for BEBs, thereby reducing the capacity of onboard batteries and effectively extending the driving range.

Although the DWC technology shows potential for reducing battery size and alleviating operation range anxiety, it is currently in the early stages of development and requires further research. Compared to the plug-in charging method, the upfront cost of the DWC facility is significantly higher, reaching 545,000 CNY/km, which is 4 times the price (Bi et al., 2018). If BEBs adopt smaller batteries, it is necessary for the system to install more DWC facilities to sustain their operation. Larger battery capacities may raise the battery cost and also impact the need for DWC facilities. The quantity of DWC facility and the battery capacity of BEBs have a mutual influence on each other. Hence, strategic planning is essential to ensure an optimal balance between battery and DWC facility costs.

The optimization of the BEB system involves several aspects. In addition to the problems of charging facility deployment and battery capacity of BEBs, it also needs to focus on the charging scheduling of BEBs. Although adopting DWC facilities can reduce the battery size, ensuring continuous service operations for BEBs generates an amount of charging demand and costs. Moreover, the irregular charging scheduling of BEBs may increase the burden on the urban power grid. To minimize the charging cost and mitigate the grid pressure, a TOU tariff mechanism has been created. It refers that the electricity price will be changed over time. The TOU tariff is usually adopted by utility companies to relieve the burden during peak hours. Thus, tactical planning should optimize the charging scheduling of BEBs under the TOU tariff by minimizing the charging cost.

To illustrate the optimization problem in this study, a framework is proposed as shown in Fig. 3. There are three decision variables in this study. The optimal deployment of DWC facilities and battery capacity constitutes a strategic planning problem, which determines the occurrence of charging activities and the maximum usable energy for BEBs. The tactical planning further optimizes the actual charging power of BEBs under the TOU tariff mechanism during the charging operations. By considering the interrelationship between strategic planning and tactical planning, an integrated planning problem can be obtained. The overarching objective of this study is to optimize the deployment of DWC facilities, battery capacity, and charging scheduling of BEBs while minimizing total costs. To specify the problem and streamline the model formulation, the following assumptions are considered:

Assumption 1. Each bus line in the system has a predetermined route, operating timetable, and fleet size of BEBs.

Assumption 2. BEBs on the same bus line have an identical battery capacity.

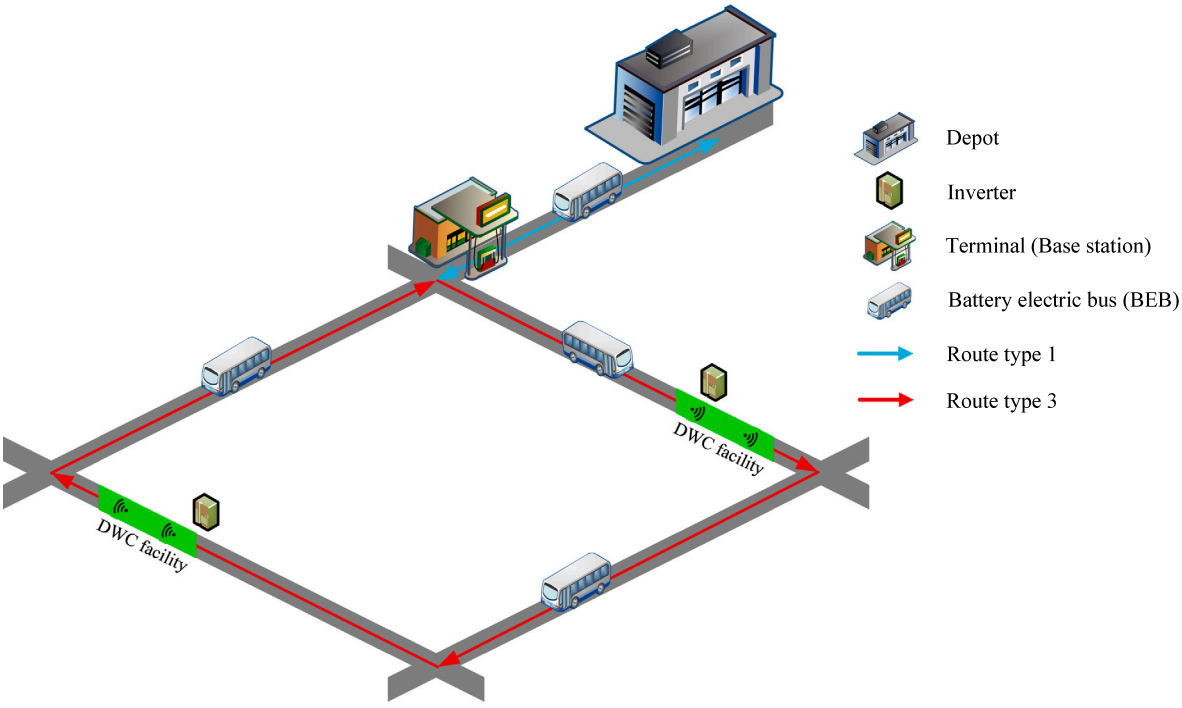

(a) An illustration of BEBs operation on the road network

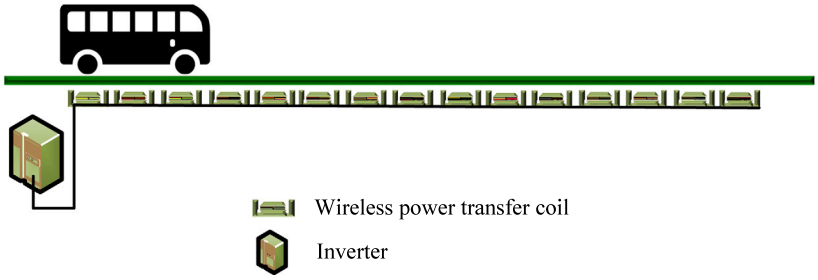

(b) A profile of the DWC facility

Fig. 2. Illustrations of the dynamic wireless charging electric bus system.

Assumption 3. The battery SOC of BEBs should be maintained within a specific range throughout their operation to preserve battery life.

Assumption 4. The charging method applied for BEBs at depots and terminals is plug-in, the DWC facilities are only deployed along the routes.

Assumption 5. BEBs can only be recharged at the depot after completing all services, and the batteries are fully charged before they start their first service trip on the next day.

Assumption 6. BEBs can select the appropriate charging power and time based on the given constraints.

Assumption 7. The energy consumption of BEBs is directly proportional to the driving distance.

Assumption 1 assumes that the fleet size and timetable of BEBs are predetermined, and BEBs will be assigned to a set of fixed trips. Assumption 2 accounts for variations in battery energy consumption due to differences in route lengths, resulting in varying battery capacity requirements. For Assumption 3, the battery SOC should be limited within a certain range to relieve damage to battery health during charging and discharging operations (He et al., 2020a). Assumption 4 states that this study only focuses on

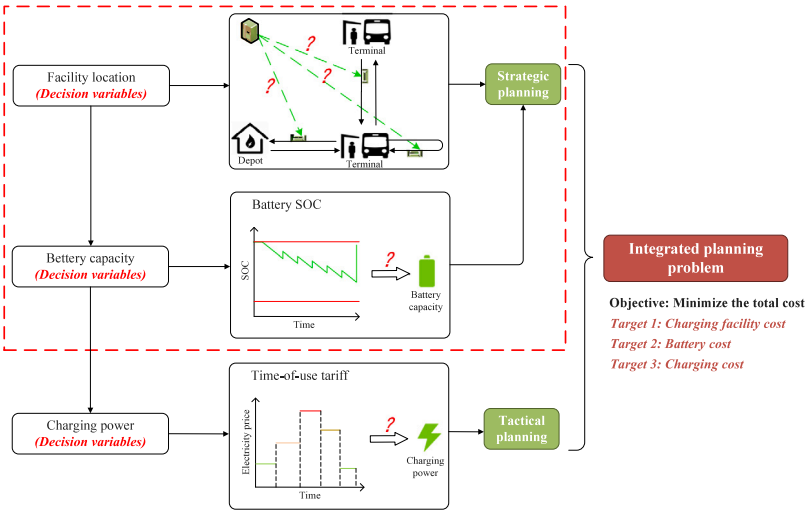

Fig. 3. Overview of the integrated optimization problem.

the deployment of DWC facilities on the routes. The implementation of DWC facilities in the BEB system requires a lengthy process of upgrades. Existing plug-in chargers should be accompanied by DWC facilities to provide battery energy replenishment for BEBs. Therefore, considering the infrastructure planning of BEB systems with multiple charging methods is reasonable (Lee et al., 2021). Additionally, this assumption relies on the principle that the DWC technology is primarily designed for charging while BEBs are in motion. BEBs stop at depots and terminals, where plug-in chargers are suitable to be used. As a result, installing DWC facilities at depots and terminals would not be practical. Assumption 5 assumes that BEBs operate under actual operating conditions to ensure normal operation and minimize energy wastage (Hwang et al., 2018). Assumption 6 states that BEBs adopt the opportunity charging strategy, which involves charging the battery at short intervals and multiple frequencies to reduce battery size. It can decrease the depth of discharge (DOD), which is a key factor in prolonging battery life (Jeong et al., 2015). Assumption 7 assumes a linear relationship between the energy consumption and operating mileage of BEBs. Similar assumptions can be found in the existing studies such as Hu et al. (2022) and Bai et al. (2022).

To make it convenient for readers to understand the proposed model, a notation table is provided in Appendix.

3. The strategic planning problem

According to Fig. 3, the primary purpose of the strategic planning problem is to optimize the deployment of the DWC facility and battery capacity of BEBs by minimizing associated costs. The strategic planning problem ensures the normal operation of BEBs under certain constraints, such as the location of DWC facilities, the residual battery energy of BEBs, and battery capacity.

3.1. Feasible region for the location of DWC facilities

To properly describe the operation process of BEBs, it first defines a feasible region for the location of DWC facilities. Let $G(N, A)$ represent the route network of the BEB system. Let N denote the set of nodes in the BEB system. To facilitate the specific location of the DWC facilities, the links of adjacent terminals are evenly divided into multiple segments. Let A be the set of segments in the BEB system. It is indexed by node pair (i, j), where i, $j \in N$ and $(i, j) \in A$. Based on Fig. 1, the route network treats one bus line as two separate directional roads. Let R denote the set of routes in the system, indexed by r. Let B_r denote all of BEBs on route r, indexed by b. For a specific BEB $b \in B_r$ on route r, let $L_{r,b}$ represent the set of service trips, indexed by l. Let D and O represent the set of depots and terminals in the system, respectively. Let $o(r) \in O$ and $d(r) \in D$ represent terminals and depots on the route $r \in R$, respectively.

To define the feasible region of the facility deployment, it should focus on the components of the DWC facility. A binary variable $X_{(i,j)}$ is introduced to determine whether the segment (i, j) is equipped by a DWC facility or not. It can be expressed in Eq. (1).

$$X_{(i,j)} = \begin{cases} 1 & \text{if segment } (i,j) \text{ is equipped by a DWC facility} \\ 0 & \text{otherwise} \end{cases} \tag{1}$$

Fig. 2(b) indicates that the DWC facility comprises inverters and wireless power transfer coils. However, the total demand for inverters in the system needs to be carefully considered. To enhance charging efficiency and reduce the facility cost, DWC facilities are usually placed continuously so that adjacent segments can share the same inverter to transmit electric power. Therefore, it is imperative to design a method for calculating the overall quantity of inverters.

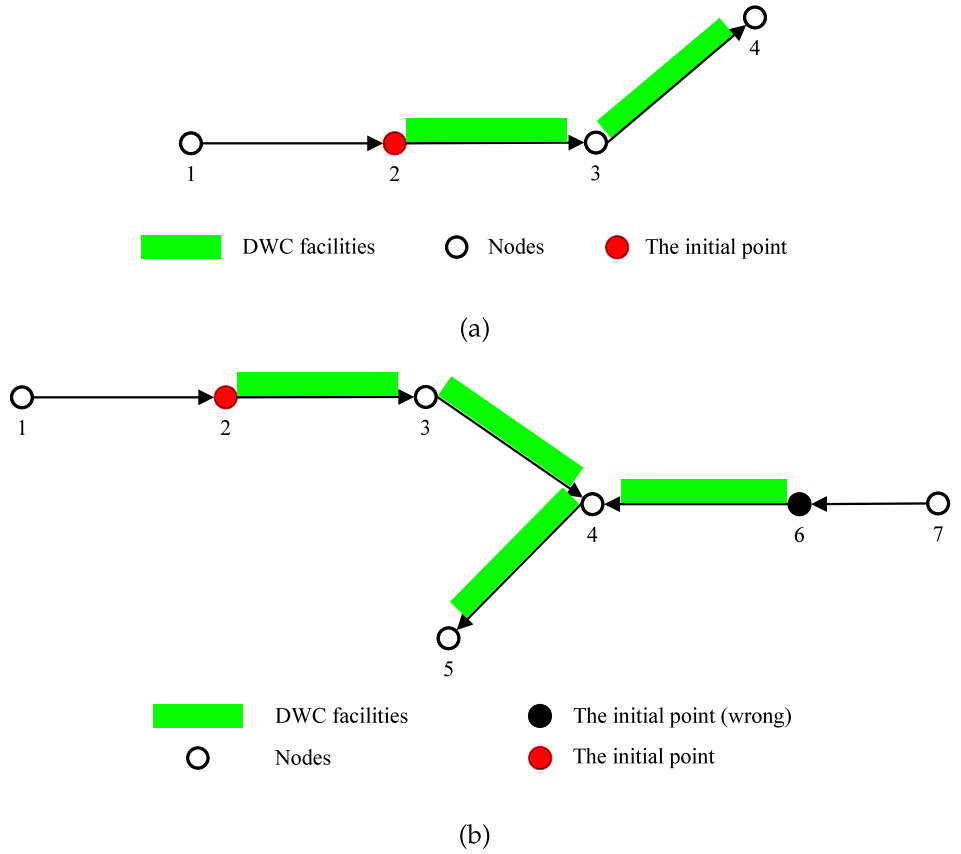

Fig. 4. Illustrations of the connections of DWC facilities.

Since adjacent segments can share the same inverter, it can identify the initial segments to calculate the total demand for inverters in the system. To determine whether the segment (i,j) is the initial segment equipped by a DWC facility or not, a binary variable $Y_{(i,j)}$ is introduced and defined in Eq. (2).

$$Y_{(i,j)} = \begin{cases} 1 & \text{if segment } (i,j) \text{ is the initial segment equipped by a DWC facility} \\ 0 & \text{otherwise} \end{cases} \tag{2}$$

Fig. 4(a) illustrates a representative example of the initial segment. One can see that segment $(2,3)$ is equipped by a DWC facility while segment $(1,2)$ is not. Based on Eq. (2), segment $(2,3)$ and node 2 are considered as the initial segment and initial point, respectively. The inverter will be installed at the node 2.

According to the Eqs. (1) and (2), the following constraints can be obtained:

$$Y_{(i,j)} \geq X_{(i,j)} - \sum_{(h,i)\in A} X_{(h,i)} \quad \forall h,i,j \in N, (i,j) \in A \tag{3}$$

$$Y_{(i,j)} \leq X_{(i,j)} \quad \forall i,j \in N, (i,j) \in A \tag{4}$$

$$Y_{(i,j)} \leq 1 - X_{(h,i)} \quad \forall h,i,j \in N, (i,j) \in A, (h,i) \in A \tag{5}$$

where (h,i) is the incoming segments of the segment (i,j).

Constraint (3) indicates that when none of the incoming segments (h,i) of segment (i,j) are equipped with DWC facilities and segment (i,j) is equipped, segment (i,j) will be defined as the initial segment. Constraint (4) ensures that if segment (i,j) has no DWC facility, it will not become the initial segment. Constraint (5) denotes that if the DWC facility installs at any incoming segment (h,i) of (i,j), then segment (i,j) will not be the initial segment.

However, not all initial segments can be considered accurately based on constraints (3)–(5). When segments intersect, the number of inverters in the system may be overestimated. As shown in Fig. 4(b), segments $(3,4)$ and segment $(6,4)$ intersect at node 4, and both are equipped with DWC facilities. Based on constraints (3)–(5), segment $(6,4)$ and node 6 will be denoted as the initial segment and initial point, respectively. However, due to the connectivity between segment $(3,4)$ and segment $(6,4)$, electric power can be transmitted accordingly. Therefore, the inverter should not be installed at node 6.

Let N^c be the set of all intersection nodes. To overcome the shortcoming, we introduce two binary variables w_i and $u_{(h,i)}$.

w_i is designed to determine whether the node $i \in N^c$ has incoming segments equipped by DWC facilities or not. It can be expressed in Eq. (6).

$$w_i = \begin{cases} 1 & \text{if incoming segments of node } i \in N^c \text{ equipped by DWC facilities} \\ 0 & \text{otherwise} \end{cases} \tag{6}$$

$u_{(h,i)}$ is introduced to determine whether the incoming segment $(h,i) \in A$ of node $i \in N^c$ has covered by inverter or not. It can be represented by Eq. (7).

$$u_{(h,i)} = \begin{cases} 1 & \text{if incoming segment } (h,i) \in A \text{ of node } i \in N^c \text{ covered by inverter} \\ 0 & \text{otherwise} \end{cases} \tag{7}$$

Based on Eq. (6) and (7), the following constraints (8)–(10) are designed to eliminate the overestimated inverters.

$$u_{(h,i)} \le X_{(h,i)} \quad \forall h \in N, i \in N^c, (h,i) \in A \tag{8}$$

$$w_i \le \sum_{(h,i)\in A} u_{(h,i)} \quad \forall i \in N^c \tag{9}$$

$$w_i \ge u_{(h,i)} \quad \forall i \in N^c, (h,i) \in A \tag{10}$$

Constraint (8) ensures that the inverter only covers segment (h,i) when the DWC facility is installed on it. Constraint (9) indicates that all inverters utilized by incoming segments of node $i \in N^c$ will be removed. Additionally, constraint (10) ensures the allocation of one inverter to the intersected segments, precisely fulfilling the requirement for energy transmission.

Based on Fig. 4(b), the total count of initial points connected to the same intersection node can be denoted as $\sum_{(h,i)\in A} u_{(h,i)}$. In practice, each junction requires only one inverter across all connected segments. The surplus number of inverters in the entire BEB system is represented by $\sum_{i\in N^c} (\sum_{(h,i)\in A} u_{(h,i)} - w_i)$.

Subsequently, by deducting redundant inverters from the overall initial count $\sum_{(i,j)\in A} Y_{(i,j)}$, the total number of inverters can be accurately calculated by the following Eq. (11).

$$Z = \sum_{(i,j)\in A} Y_{(i,j)} - \sum_{i\in N^c} \sum_{(h,i)\in A} u_{(h,i)} + \sum_{i\in N^c} w_i \tag{11}$$

where Z is the total demand for inverters within the BEB system.

Finally, constraints (12)–(15) ensure that $X_{(i,j)}$, $Y_{(i,j)}$, $u_{(h,i)}$, and w_i are binary variables, respectively.

$$X_{(i,j)} \in \{0,1\} \tag{12}$$

$$Y_{(i,j)} \in \{0,1\} \tag{13}$$

$$u_{(h,i)} \in \{0,1\} \tag{14}$$

$$w_i \in \{0,1\} \tag{15}$$

3.2. Feasible region for the battery capacity of BEBs

To define the feasible region for the battery capacity of BEBs, it is essential to consider the residual battery energy of BEBs throughout their entire service cycles. The feasible region for the battery capacity is a critical constraint to the infrastructure planning problem. It ensures that the BEB system operates normally while minimizing the battery cost. Figs. 5(a) and 5(b) demonstrate the operation of BEBs and the variations in their residual battery energy, using Route types 1 and 3 as an example.

Let $e^+_{r,b,d}$ represent the residual battery energy as BEB $b \in B_r$ leaves from the depot $d\,(r)$ on route r. Before the BEB starts the first service trip, it reaches Terminal 1 (base station) with energy consumption of $c_{r,b,(d,o)}$. Let $e^+_{r,b,l,o}$ represent the residual battery energy of BEB $b \in B_r$ as it leaves the terminal $o\,(r)$ on route r in service trip $l \in L_{r,b}$. Similarly, let $e_{r,b,l,i}$ express the residual battery energy of BEB $b \in B_r$ on route r as it reaches node i in service trip $l \in L_{r,b}$. Let $s_{r,b,l,(i,j)}$ and $c_{r,b,l,(i,j)}$ denote the battery energy replenished and consumed by BEB $b \in B_r$ on route r as it passes the segment (i,j) in the service trip $l \in L_{r,b}$, respectively. After completing its first service trip, BEBs will return to Terminal 1 (base station). Let $e^-_{r,b,l,o}$ represent the residual battery energy of BEB $b \in B_r$ as it reaches the terminal $o\,(r)$ on route r in service trip $l \in L_{r,b}$. Because the terminal is equipped with plug-in chargers, BEBs can be charged during layovers between adjacent service trips. We use variable $s_{r,b,l,o}$ to represent the battery energy replenished by BEB $b \in B_r$ as it idles in terminal $o\,(r)$ on route r in service trip $l \in L_{r,b}$. Then, BEBs will repeat the service process in accordance with the timetable. Instead of charging at the terminal, BEBs will return to the depot as it finishes the last service trip. Let $l^{\Omega}_{r,b}$ represent the last service trip for BEB $b \in B_r$ on route r. Let $e^-_{r,b,d}$ represent the residual battery energy as BEB $b \in B_r$ on route r returns to the depot $d\,(r)$, and the energy consumption during the return trip is $c_{r,b,(o,d)}$. BEBs will utilize the nighttime to charge at the depot. Let $s_{r,b,d}$ represent the battery energy replenished by BEB $b \in B_r$ as it idles in depot $d\,(r)$ on route r during the last service trip. According to Assumption 5, BEBs will be fully charged and prepared for the next day at the depot.

The energy fluctuations of BEBs during their operations can be represented using the following constraints:

$$e^+_{r,b,d} = e^-_{r,b,d} + s_{r,b,d} = \varepsilon^+ E_r \quad \forall r \in R, b \in B_r, d = d\,(r) \tag{16}$$

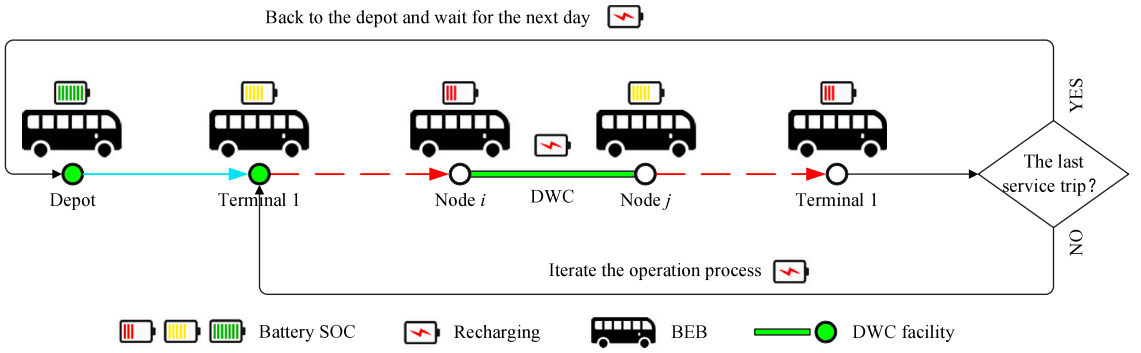

(a) An illustration of the whole operation process of BEB

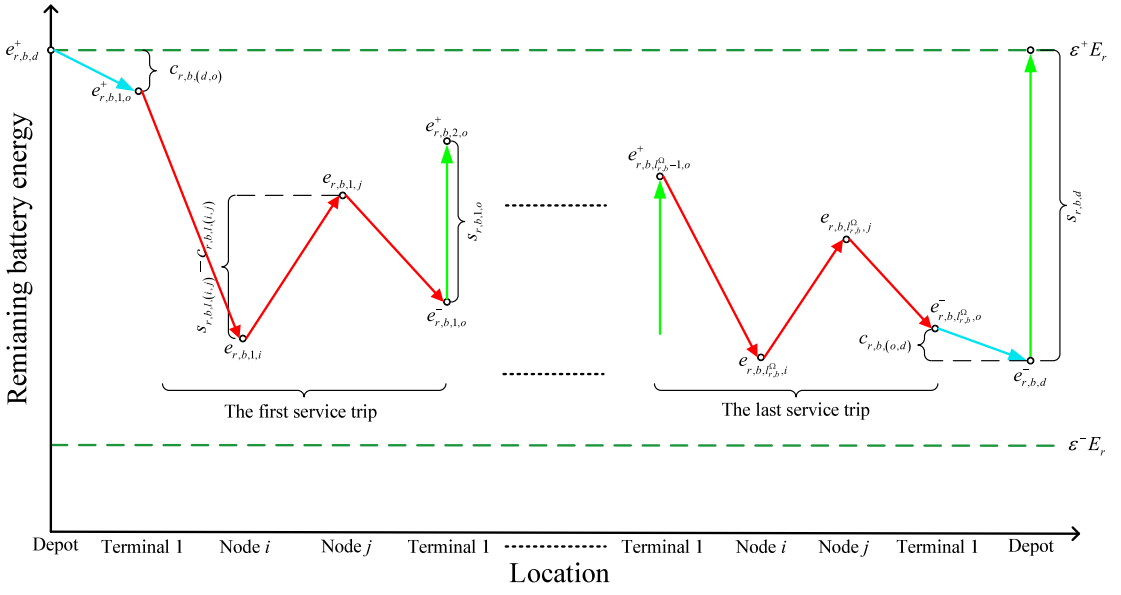

(b) An illustration of changes in the residual battery energy of BEBs

Fig. 5. Illustrations of battery energy changes during operation.

$$e^{+}_{r,b,l,o} = e^{+}_{r,b,d} - c_{r,b,(d,o)} \quad \forall r \in R, b \in B_r, l = 1, o = o_b(r), d = d(r) \tag{17}$$

$$e_{r,b,l,j} = e_{r,b,l,i} - c_{r,b,l,(i,j)} + s_{r,b,l,(i,j)} \quad \forall r \in R, b \in B_r, l \in L_{r,b}, i, j \in N_r, (i,j) \in A_r \tag{18}$$

$$e^{+}_{r,b,l,o} = e^{-}_{r,b,l-1,o} + s_{r,b,l-1,o} \quad \forall r \in R, b \in B_r, l \in L_{r,b}, o = o_b(r), l \geq 2 \tag{19}$$

$$e^{+}_{r,b,l,o} = e^{-}_{r,b,l,o} + s_{r,b,l,o} \quad \forall r \in R, b \in B_r, l \in L_{r,b}, o \in o(r) \setminus o_b(r) \tag{20}$$

$$e^{-}_{r,b,d} = e^{-}_{r,b,l,o} - c_{r,b,(o,d)} \quad \forall r \in R, b \in B_r, l = l^{\Omega}_{r,b}, d = d(r), o = o_b(r) \tag{21}$$

$$0 \leq s_{r,b,l,(i,j)} \leq \alpha X_{(i,j)} P^{\max 1} t_{r,b,l,(i,j)} \quad \forall r \in R, b \in B_r, l \in L_{r,b}, i, j \in N_r, (i,j) \in A_r \tag{22}$$

$$0 \leq s_{r,b,l,o} \leq \beta P^{\max 2} t_{r,b,l,o} \quad \forall r \in R, b \in B_r, l \in L_{r,b}, o = o(r) \tag{23}$$

$$0 \leq s_{r,b,d} \leq \beta P^{\max 2} t_{r,b,d} \quad \forall r \in R, b \in B_r, d = d(r) \tag{24}$$

$$\varepsilon^{-} E_r \leq e^{-}_{r,b,d} \leq \varepsilon^{+} E_r \quad \forall r \in R, b \in B_r, d = d(r) \tag{25}$$

$$\varepsilon^{-} E_r \leq e^{-}_{r,b,l,o} \leq \varepsilon^{+} E_r \quad \forall r \in R, b \in B_r, l \in L_{r,b}, o = o(r) \tag{26}$$

$$\varepsilon^{-} E_r \leq e^{+}_{r,b,l,o} \leq \varepsilon^{+} E_r \quad \forall r \in R, b \in B_r, l \in L_{r,b}, o = o(r) \tag{27}$$

$$\varepsilon^- E_r \le e_{r,b,l,i} \le \varepsilon^+ E_r \quad \forall r \in R, b \in B_r, l \in L_{r,b}, i \in N_r \tag{28}$$

where A_r denotes the set of all segments on route r, and $A_r \subseteq A$; N_r denotes the set of all nodes on route r, $N_r \subseteq N$; $o_b(r)$ denotes the base station on route r, $o_b(r) \subseteq o(r)$; $P^{\max 1}$ and $P^{\max 2}$ denote the nominal charging power for the DWC facility and plug-in charger, respectively; $t_{r,b,l,(i,j)}$ is the travel time as BEB $b \in B_r$ passes through the segment (i,j) on route r; $t_{r,b,l,o}$ and $t_{r,b,d}$ are the layover time of the BEB $b \in B_r$ as it idles in terminal $o(r)$ and depot $d(r)$ on route r, respectively; α and β are the charging efficiencies of the DWC facility and plug-in charger, and $0 < \alpha < \beta < 1$, respectively; ε^- and ε^+ are the lower and upper boundaries of battery SOC, and $0 < \varepsilon^- < \varepsilon^+ < 1$, respectively; E_r represents the battery size of BEBs on route r.

Constraint (16) indicates that the battery of BEBs should be at full charge when they start the first service trip from the depot. Constraint (17) represents the consumption of battery energy when they start from the depot to the terminal in the first service trip. The battery energy change of the BEBs from nodes i to j is represented by constraint (18). Constraint (19) indicates that the BEBs can obtain battery energy when they idle in the base station. Constraint (20) denotes the battery energy replenished by BEBs due to charging at terminals (excluding the base station). When BEBs complete their service trips and return to the depot, the battery energy consumed is captured by constraint (21). To limit the amount of battery energy that can be obtained by BEBs at any location, constraint (22) specifies maximum thresholds for replenished battery energy at segments (i,j). It is represented by $\alpha X_{(i,j)} P^{\max 1} t_{r,b,l,(i,j)}$. Similarly, constraints (23) and (24) describe the battery energy replenished by BEBs when they charge at terminals (including base station) and depot should not exceed the maximum thresholds, respectively. Constraints (25)–(28) ensure that the residual battery energy of BEBs at any location should be restricted to a certain range of battery capacity based on Assumption 3.

The battery capacity of BEBs on route r is treated as a variable in this paper. As the battery size changes, the weight of BEBs is correspondingly altered. Given that the battery consumption of BEBs is influenced by the vehicle weight, changes in battery capacity will accordingly affect the battery consumption. To determine the relationship between the battery size and battery consumption of BEBs, let $\widehat{\Delta c_r}$ denote the battery consumption per kilometer for BEBs on route r. Referring to the research results presented by Bi et al. (2015), a 10% reduction in the weight of BEBs corresponds to a 4.5% reduction in battery consumption. Therefore, we can express Eq. (29) as follows:

$$\widehat{\Delta c_r} = \left[1 - \frac{\frac{(E^{bus} - E_r)}{\rho}}{(W^{bus} + W^{extra})} \times \frac{4.5\%}{10\%}\right] \Delta c \quad \forall r \in R \tag{29}$$

where W^{bus} and E^{bus} denote the curb weight and the nominal battery capacity of BEBs, respectively; ρ denotes the energy density of the battery; Δc represents the baseline battery consumption of BEBs. The benchmark values of W^{bus} and E^{bus} are taken from the Foton electric buses used in Beijing, whose curb weight is 11,600 kg, featuring a lithium–iron–phosphate battery with a capacity of 326.73 kWh (Foton, 2022). The passenger weight of BEBs is denoted as W^{extra} and is assumed to be 1000 kg. According to Chen et al. (2018), the energy density ρ is valued at 0.17 kWh/kg. The baseline battery consumption Δc is set as 1.42 kWh/km, which is estimated in Ma et al. (2021).

Based on Eq. (29) and Assumption 7, the variables $c_{r,b,l,(i,j)}$, $c_{r,b,(o,d)}$, and $c_{r,b,(d,o)}$ can be further elucidated using Eqs. (30)–(32), as follows:

$$c_{r,b,l,(i,j)} = l_{(i,j)} \left[1 - \frac{\frac{(E^{bus} - E_r)}{\rho}}{(W^{bus} + W^{extra})} \times 0.45\right] \Delta c \quad \forall r \in R, b \in B_r, l \in L_{r,b}, (i,j) \in A_r \tag{30}$$

$$c_{r,b,(o,d)} = l_{(o,d)} \left[1 - \frac{\frac{(E^{bus} - E_r)}{\rho}}{(W^{bus} + W^{extra})} \times 0.45\right] \Delta c \quad \forall r \in R, b \in B_r, o = o_b(r), d = d(r) \tag{31}$$

$$c_{r,b,(d,o)} = l_{(d,o)} \left[1 - \frac{\frac{(E^{bus} - E_r)}{\rho}}{(W^{bus} + W^{extra})} \times 0.45\right] \Delta c \quad \forall r \in R, b \in B_r, o = o_b(r), d = d(r) \tag{32}$$

where $l_{(i,j)}$, $l_{(o,d)}$, and $l_{(d,o)}$ represent the length of segment (i,j), the distance from the base station $o_b(r)$ to the depot $d(r)$, and the distance from the depot $d(r)$ to the base station $o_b(r)$, respectively.

In summary, the feasible region for the deployment of DWC facilities and the battery capacity of BEBs is referred to as Θ hereafter.

Let M_1 and M_2 denote the cost of DWC facilities and batteries, respectively. The optimal deployment of DWC facilities and battery capacity of BEBs can be determined by minimizing the total cost. The following program P1 can be expressed as a formulation of the strategic planning problem.

P1:

$$\begin{aligned} &\min(M_1 + M_2) = Z q^{inv} + \sum_{(i,j)\in A} X_{(i,j)} q^{coil} \Delta l + \sum_{r \in R} \eta_r E_r q^{bat} \\ &s.t. \quad X_{(i,j)}, E_r \in \Theta \end{aligned} \tag{33}$$

where q^{inv}, q^{coil}, and q^{bat} are the unit cost of the inverter, wireless power transfer coils, and battery, respectively; Δl is the unit length of the segment. η_r is the fleet size of the BEBs on route $r \in R$.

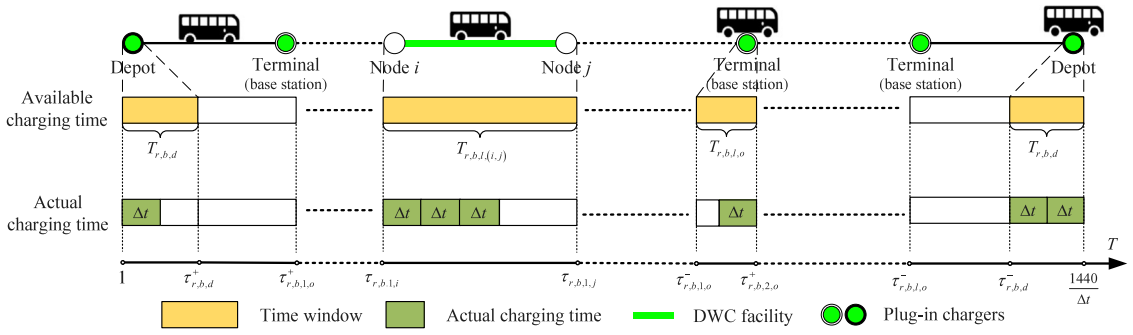

Fig. 6. The charging time windows of BEBs for a whole day.

The cost of DWC facilities is comprised of inverters and transfer coils, as shown in Fig. 2(b). The cost of coils varies depending on the total number (length) of DWC facilities. It is represented by $\sum_{(i,j)\in A} X_{(i,j)} q^{coil} \Delta l$. Based on Eq. (10), the cost of inverters can be represented by Zq^{inv}. In addition, the total battery cost is computed based on the battery capacity of BEBs E_r and the fleet size of BEBs η_r on a specific route, represented as $\sum_{r\in R} \eta_r E_r q^{bat}$.

4. The tactical planning problem

As a segment is equipped with a DWC facility, a set of available charging time windows is generated. It also uses Route types 1 and 3 as an example to represent the charging time windows of BEBs as shown in Fig. 6. Based on constraints (25)–(28), the residual battery energy should be restricted between $\varepsilon^- E_r$ to $\varepsilon^+ E_r$ throughout the operation processes of BEBs. As the battery energy of BEBs is full, they will not receive any additional energy, even during the available charging time windows. Conversely, if the residual battery energy of BEBs is insufficient to complete the journey, they will be charged in the available charging time windows. The time windows provide BEBs with the opportunity to charge throughout the designated periods. However, the charging activities of BEBs are uncertain due to the infrastructure planning problem. To determine the actual charging time and energy replenishment of BEBs, it should focus on the charging scheduling of BEBs in the feasible region.

Within the defined feasible region, the solutions do not incorporate the charging scheduling of BEBs. The disorderly charging scheduling may incur more charging costs due to the undulated electricity price caused by the TOU tariff. Therefore, the optimization of charging scheduling for BEBs can be achieved by minimizing the charging cost. To calculate the cost, the charging activities of BEBs can be decomposed based on time intervals. Let Δt denote the length of a time interval. Since one day consists of 1440 min, it can be evenly divided into intervals of Δt. Let T represent the set of time intervals within one day, where $T = \left\{1, 2, \ldots, \frac{1440}{\Delta t}\right\}$. The charging cost is determined by the charging power, as the electricity price and charging time are regarded as constant in each time interval. Therefore, optimizing the charging scheduling of BEBs under the TOU tariff mechanism entails further constraints within the defined feasible region in terms of charging power.

Based on Fig. 6, the operation process of BEBs can be rephrased in respect of time windows. BEBs should be fully charged and depart from the depot. Let $T_{r,b,d}$ denote the set of available charging time windows when BEB $b \in B_r$ idles in depot $d(r)$ on route r. Let $\tau^+_{r,b,d}$ represent the moment when BEB $b \in B_r$ leaves the depot $d(r)$ on route r. Then, BEBs will arrive at the terminal (base station). Let $T_{r,b,l,o}$ represent the set of available charging time windows when BEB $b \in B_r$ idles in terminal $o(r)$ on route r in service trip $l \in L_{r,b}$. Let $\tau^-_{r,b,l,o}$ and $\tau^+_{r,b,l,o}$ express the moment when BEB $b \in B_r$ reaches and leaves terminal $o(r)$ on route r in service trip $l \in L_{r,b}$, respectively. BEBs have the opportunity to recharge their batteries as they pass through segments equipped with DWC facilities. Let $T_{r,b,l,(i,j)}$ indicate the set of available charging time windows when BEB $b \in B_r$ passes through the segment (i,j) in service trip $l \in L_{r,b}$. Similarly, let $\tau_{r,b,l,i}$ and $\tau_{r,b,l,j}$ denote the moment when BEB $b \in B_r$ on route r arrives and leaves the node i and node j in service trip $l \in L_{r,b}$, respectively. After completing their final service trip, BEBs will repeat the service process and return to the depot. Let $\tau^-_{r,b,d}$ denote the moment when BEB $b \in B_r$ returns to the depot $d(r)$ on route r. The following constraints should be satisfied:

$$P_{r,b,l,t,(i,j)} = 0 \quad \forall r \in R, b \in B_r, l \in L_{r,b}, (i,j) \in A_r, t \notin T_{r,b,l,(i,j)} \tag{34}$$

$$X_{(i,j)} P_{r,b,l,t,(i,j)} \geq 0 \quad \forall r \in R, b \in B_r, l \in L_{r,b}, (i,j) \in A_r, t \in T_{r,b,l,(i,j)} \tag{35}$$

$$P_{r,b,l,o,t} = 0 \quad \forall r \in R, b \in B_r, l \in L_{r,b}, o = o(r), t \notin T_{r,b,l,o} \tag{36}$$

$$P_{r,b,l,o,t} \geq 0 \quad \forall r \in R, b \in B_r, l \in L_{r,b}, o = o(r), t \in T \tag{37}$$

$$P_{r,b,d,t} = 0 \quad \forall r \in R, b \in B_r, d = d(r), t \notin T_{r,b,d} \tag{38}$$

$$P_{r,b,d,t} \geq 0 \quad \forall r \in R, b \in B_r, d = d(r), t \in T \tag{39}$$

$$P_{r,b,l,t,(i,j)} \leq P^{\max 1} \quad \forall r \in R, b \in B_r, l \in L_{r,b}, (i,j) \in A_r, t \in T_{r,b,l,(i,j)} \tag{40}$$

$$P_{r,b,l,o,t} \le P^{\max 2} \quad \forall r \in R, b \in B_r, l \in L_{r,b}, o = o(r), t \in T_{r,b,l,o} \tag{41}$$

$$P_{r,b,d,t} \le P^{\max 2} \quad \forall r \in R, b \in B_r, d = d(r), t \in T_{r,b,d} \tag{42}$$

$$s_{r,b,l,(i,j)} = \sum_{t \in T_{r,b,l,(i,j)}} \alpha X_{(i,j)} P_{r,b,l,t,(i,j)} \Delta t \quad \forall r \in R, b \in B_r, l \in L_{r,b}, (i,j) \in A_r \tag{43}$$

$$s_{r,b,l,o} = \sum_{t \in T_{r,b,l,o}} \beta P_{r,b,l,o,t} \Delta t \quad \forall r \in R, b \in B_r, l \in L_{r,b}, o = o(r) \tag{44}$$

$$s_{r,b,d} = \sum_{t \in T_{r,b,d}} \beta P_{r,b,d,t} \Delta t \quad \forall r \in R, b \in B_r, d = d(r) \tag{45}$$

where $P_{r,b,l,t,(i,j)}$, $P_{r,b,l,o,t}$, and $P_{r,b,d,t}$ are the actual charging power of the BEB $b \in B_r$ on route r at the time $t \in T$ as it locates at the segment (i,j), terminal $o(r)$, and depot $d(r)$, respectively.

Constraints (34) and (35) stipulate that BEBs can only replenish battery energy when driving on the segments (i,j) equipped with a DWC facility. Furthermore, BEBs can select appropriate charging power by utilizing the opportunity charging strategy as specified in Assumption 6. Constraints (36) and (37) ensure that the charging power of BEBs is positive when BEBs charge at terminals $o(r)$ during layover between adjacent service trips. Similarly, the BEBs cannot obtain battery energy if they are not dwelling at the depots, and the charging power is variable and positive as shown in constraints (38) and (39). Constraints (40)–(42) ensure that the actual charging power rate of BEBs cannot exceed the nominal value of the DWC facility and plug-in charger respectively. Constraints (43)–(45) denote that the total amount of battery energy replenished by BEBs when they are located at the segment (i,j), terminal $o(r)$, and depot $d(r)$, respectively.

In summary, we can formulate a program P2 to calculate the total charging costs:

P2:

$$\begin{aligned} \min M_3 = & \sum_{r \in R} \sum_{b \in B_r} \sum_{o=o(r)} \sum_{t \in T_{r,b,o}} \beta q_t P_{r,b,l,o,t} \Delta t + \sum_{r \in R} \sum_{b \in B_r} \sum_{d=d(r)} \sum_{t \in T_{r,b,d}} \beta q_t P_{r,b,d,t} \Delta t \\ & + \sum_{r \in R} \sum_{b \in B_r} \sum_{(i,j) \in A_r} \sum_{t \in T_{r,b,l,(i,j)}} \alpha q_t X_{(i,j)} P_{r,b,l,t,(i,j)} \Delta t \end{aligned} \tag{46}$$

$$s.t. \quad \text{Constraints (16)–(32) and (34)–(45)}$$

where M_3 is the total charging cost generated by all BEBs in the system.

5. Integrated planning problem

5.1. Optimization model

Combining the programs P1, P2, and the defined feasible region, the DWC facility deployment, battery capacity, and charging schedule of BEBs considering the TOU tariff problems can be formulated in the integrated program P3:

P3:

$$\begin{aligned} \min M_{total} = & Z q^{inv} + \sum_{(i,j) \in A} X_{(i,j)} q^{coil} \Delta l + \sum_{r \in R} \eta_r E_r q^{bat} \\ & + \sum_{r \in R} \sum_{b \in B_r} \sum_{(i,j) \in A_r} \sum_{t \in T_{r,b,l,(i,j)}} \alpha q_t X_{(i,j)} P_{r,b,l,t,(i,j)} \Delta t \\ & + \sum_{r \in R} \sum_{b \in B_r} \sum_{o=o(r)} \sum_{t \in T_{r,b,l,o}} \beta q_t P_{r,b,l,o,t} \Delta t \\ & + \sum_{r \in R} \sum_{b \in B_r} \sum_{d=d(r)} \sum_{t \in T_{r,b,d}} \beta q_t P_{r,b,d,t} \Delta t \end{aligned} \tag{47}$$

$$s.t. \quad X_{(i,j)}, E_r \in \Theta$$

Constraints (34)–(45)

where M_{total} represents the overall cost of the BEB system, derived from the summation of M_1, M_2, and M_3.

The proposed integrated optimization model is an MINLP because the nonlinear term $X_{(i,j)} P_{r,b,l,t,(i,j)}$ exists in the objective function, constraint (35), and constraint (43). It is a typical NP-hard problem, making it challenging to find efficient solutions directly using normal algorithms or solvers. To solve the MINLP problem, it is essential to reformulate the proposed model.

5.2. Model linearization

As mentioned above, the proposed model P3 has a nonlinear term $X_{(i,j)} P_{r,b,l,t,(i,j)}$. To eliminate the nonlinearity of the proposed integrated model, an auxiliary variable $\hat{P}_{r,b,l,t,(i,j)}$ is introduced. The relationship between the auxiliary variable and the nonlinear term is as follows:

$$\hat{P}_{r,b,l,t,(i,j)} = X_{(i,j)} P_{r,b,l,t,(i,j)} \quad \forall r \in R, b \in B_r, l \in L_{r,b}, (i,j) \in A_r, t \in T_{r,b,l,(i,j)} \tag{48}$$

In the nonlinear term, the nonnegative variable $P_{r,b,l,t,(i,j)}$ is defined within the domain of $\left[0, P^{\max 1}\right]$. According to Eq. (1), the variable $X_{(i,j)}$ is a binary variable. Therefore, $\hat{P}_{r,b,l,t,(i,j)}$ must adhere to the following constraint (49).

$$\hat{P}_{r,b,l,t,(i,j)} \leqslant X_{(i,j)} P^{\max 1} \quad \forall r \in R, b \in B_r, l \in L_{r,b}, (i,j) \in A_r, t \in T_{r,b,l,(i,j)} \tag{49}$$

In addition, $\hat{P}_{r,b,l,t,(i,j)}$ should comply the following constraints (50)–(51).

$$\hat{P}_{r,b,l,t,(i,j)} \leqslant P_{r,b,l,t,(i,j)} \quad \forall r \in R, b \in B_r, l \in L_{r,b}, (i,j) \in A_r, t \in T_{r,b,l,(i,j)} \tag{50}$$

$$\hat{P}_{r,b,l,t,(i,j)} \geqslant P_{r,b,l,t,(i,j)} - P^{\max 1}\left[1 - X_{(i,j)}\right] \quad \forall r \in R, b \in B_r, l \in L_{r,b}, (i,j) \in A_r, t \in T_{r,b,l,(i,j)} \tag{51}$$

By replacing the nonlinear term $X_{(i,j)} P_{r,b,l,t,(i,j)}$ with $\hat{P}_{r,b,l,t,(i,j)}$, the nonlinear constraints (35) and (43) are reformulated as the following linear constraints:

$$\hat{P}_{r,b,l,t,(i,j)} \geq 0 \quad \forall r \in R, b \in B_r, l \in L_{r,b}, (i,j) \in A_r, t \in T_{r,b,l,(i,j)} \tag{52}$$

$$s_{r,b,l,(i,j)} = \sum_{t \in T_{r,b,l,(i,j)}} \hat{P}_{r,b,l,t,(i,j)} \Delta t \quad \forall r \in R, b \in B_r, l \in L_{r,b}, (i,j) \in A_r \tag{53}$$

Finally, the original integrated optimization model P3 can be transformed into the linearized MILP P4, as illustrated below:

P4:

$$\begin{aligned} \min M_{total} = {} & Z q^{inv} + \sum_{(i,j) \in A} X_{(i,j)} q^{coil} \Delta l + \sum_{r \in R} \eta_r E_r q^{bat} \\ & + \sum_{r \in R} \sum_{b \in B_r} \sum_{(i,j) \in A_r} \sum_{t \in T_{r,b,l,(i,j)}} \alpha q_t \hat{P}_{r,b,l,t,(i,j)} \Delta t \\ & + \sum_{r \in R} \sum_{b \in B_r} \sum_{o = o(r)} \sum_{t \in T_{r,b,l,o}} \beta q_t P_{r,b,l,o,t} \Delta t \\ & + \sum_{r \in R} \sum_{b \in B_r} \sum_{d = d(r)} \sum_{t \in T_{r,b,d}} \beta q_t P_{r,b,d,t} \Delta t \end{aligned} \tag{54}$$

$$s.t. \quad X_{(i,j)}, E_r \in \Theta$$

Constraints (34), (36)–(42), (44)–(45), and (48)–(53)

Subsequently, we will demonstrate the equivalence between P4 and the original model P3. Since $X_{(i,j)}$ is the binary variable, two scenarios can be discussed based on the possible values of $X_{(i,j)}$.

Scenario 1: $X_{(i,j)} = 1$

When $X_{(i,j)} = 1$, it is obvious that $\hat{P}_{r,b,l,t,(i,j)} = P_{r,b,l,t,(i,j)}$, based on the definition of $\hat{P}_{r,b,l,t,(i,j)}$, i.e., constraint (48). Therefore, constraint (50) is always satisfied under this scenario. To eliminate the possibility that $\hat{P}_{r,b,l,t,(i,j)} < P_{r,b,l,t,(i,j)}$ in constraint (50), it is necessary to add another constraint, which is constraint (51), to ensure that $\hat{P}_{r,b,l,t,(i,j)} = P_{r,b,l,t,(i,j)}$. Constraint (50), together with constraint (51), can ensure that constraint (48) is always satisfied under the scenario when $X_{(i,j)} = 1$.

Scenario 2: $X_{(i,j)} = 0$

When $X_{(i,j)} = 0$, according to constraint (48), $\hat{P}_{r,b,l,t,(i,j)} = 0$. And when $X_{(i,j)} = 0$, it indicates that segment (i,j) is not equipped with the DWC facility, and BEBs cannot be charged on segment (i,j), which means $P_{r,b,l,t,(i,j)} = 0$. Therefore, constraint (50) is always satisfied under this scenario.

For constraint (51), when $X_{(i,j)} = 0$, the left side of this constraint $\hat{P}_{r,b,l,t,(i,j)}$ equals 0; the right side of this constraint equals $-P^{\max 1}$, which is a negative value. Therefore, constraint (51) is also satisfied under this scenario.

Based on the above discussion, we can see that under constraints (49)–(51), the nonlinear term $X_{(i,j)} P_{r,b,l,t,(i,j)}$ can be equivalently replaced by $\hat{P}_{r,b,l,t,(i,j)}$. Therefore, P4 is equivalent to P3.

6. Numerical studies

To validate the efficiency of the optimized model, we conducted numerical studies using an actual bus system in Beijing, China. Section 6.1 provides the basic information about the BEB system and determines the parameter values used in the model. Section 6.2 demonstrates and explains the results obtained from solving the optimization model. Sensitivity analysis of key parameters that influence the optimization results is conducted in Section 6.3.

6.1. Bus system description and model parameters

The selected three routes are Route 19 (green), Route 56 (yellow), and Route 65 (blue) in the BEB system of Beijing, as illustrated in Fig. 7. To provide a depiction of each route and simplify route delineation, Fig. 8 illustrates the topological structure of the system. Table 1 provides specific links to each route. It can be observed that the three routes of the system share a common base station and depot, denoted as node 1 and the Depot in Fig. 8, respectively. Additionally, Route 56 is a circular route with its initial and ending point at the base station. Table 2 summarizes the information on these three bus routes, including route length, fleet size, operation time, departure intervals, and total number of service trips.

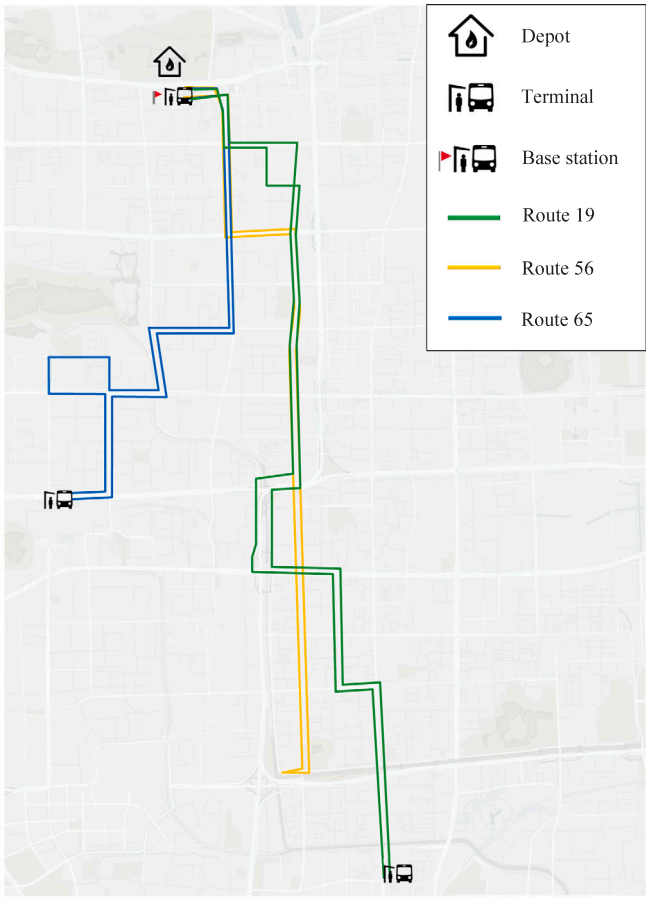

Fig. 7. Map of the bus system.

Table 1
Bus route links.

Route number	Links
19	1→ 2 → 3 → 5 → 7 → 17 → 18 → 21 → 22 → 23 → 24 → 25 → 32→ 33 → 34 → 35 → 36 → 37 → 38 → 40 → 41 → 42 → 43 → 44 →1
56	1→ 2 → 3 → 4 → 7 → 17 → 19 → 20 → 31 → 37 → 38 → 39 → 43 → 44 →1
65	1→ 2 → 3 → 4 → 6 → 8 → 9 → 10 → 11 → 12 → 13 → 14 → 15 → 16 → 26→ 27 → 28 → 29 → 30 → 39 → 43 → 44 →1

Table 2
Fundamental information about bus routes.

Route number	Length (km)	Fleet size	Operation hours	Departure interval (minutes)	Number of service trips
19	22.6	15	5:00–24:00	10	131
56	17.6	9	5:30–23:00	10	82
65	15.6	13	5:00–23:00	10	110

The schedule of the TOU tariff in Beijing is shown in Table 3. It reveals a pattern of lower charging costs during the night hours (23:00 to 7:00) and higher costs during midday and evening hours (10:00 to 15:00 and 18:00 to 21:00). Additionally, the existing peak charging costs are further increased during July and August (11:00 to 13:00 and 16:00 to 17:00), reaching 1.422 CNY/kWh.

The values of the remaining crucial parameters are displayed in Table 4. The battery cost is set at 750 CNY/kWh, while the costs for the inverter and coils of the DWC facility are 45,000 CNY per unit and 500 CNY/m, respectively. These values are adopted from the studies by Wang et al. (2022), Bi et al. (2018), and Cirimele et al. (2018). Based on the research of An (2020) and Rupp et al. (2020), the lifespan of the DWC charging facility and battery is assumed to be 10 years and 6 years, respectively. Amortized costs are calculated by spreading the costs of batteries and DWC facilities over their respective lifespans. According to the studies

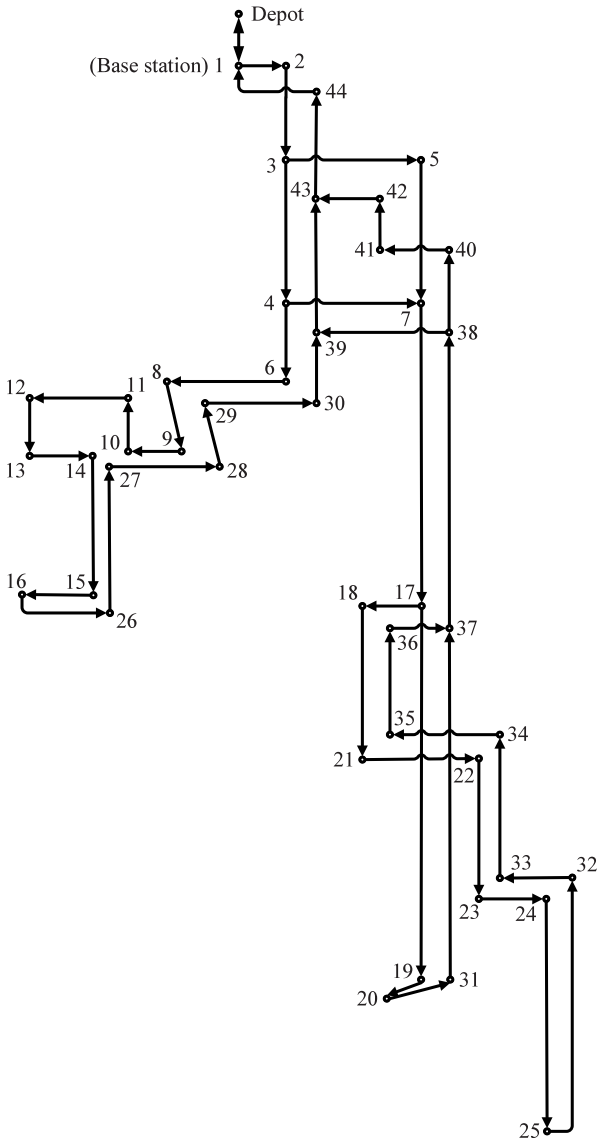

Fig. 8. Topological structure of the BEB system.

Table 3
The TOU tariff information schedule.

	Time periods	Electricity price (CNY/kWh)
Valley time	23:00–7:00	0.294
	7:00–10:00	
Flat time	15:00–18:00	0.767
	21:00–23:00	
Peak time	10:00–15:00	1.293
	18:00–21:00	
	11:00–13:00	1.422[a]
	16:00–17:00	

[a] Note: The special peak electricity price is applicable only during July and August each year.

conducted by Liu and Song (2017) and He et al. (2022a), the nominal charging powers of BEBs at the DWC facility and plug-in charger are valued at 80 kW and 10 kW, respectively. The assumed charging efficiencies for DWC facilities and plug-in chargers are

Table 4
Model parameters.

Parameters	Symbols	Values	References
Amortized battery cost (CNY/kWh)	q^{bat}	125	Wang et al. (2022)
Amortized cost of the inverter per unit (CNY)	q^{inv}	4500	Bi et al. (2018)
Amortized cost of the transfer coil (CNY/m)	q^{coil}	50	Cirimele et al. (2018)
Nominal charging power of DWC facility (kW)	$P^{\max 1}$	80	Liu and Song (2017)
Nominal charging power of plug-in charger (kW)	$P^{\max 2}$	10	He et al. (2022a)
The charging efficiency rate of DWC facility	α	85%	Bi et al. (2018)
The charging efficiency rate of plug-in facility	β	90%	He et al. (2020a)
The upper bound of battery SOC	ε^{+}	90%	He et al. (2022a)
The lower bound of battery SOC	ε^{-}	20%	Hwang et al. (2018)
Battery service life (year)	/	6	Rupp et al. (2020)
DWC facility service life (year)	/	10	An (2020)
The length of unit time interval (minutes)	Δt	1	/
The length of unit segment (m)	Δl	400	/

Table 5
Comparison of results between the optimal and limited models.

Item		Optimal model	Limited model
Total cost (CNY)		2,920,675.40	3,249,556.24
Charging facility cost (CNY)		337,000.00	317,000.00
Battery cost (CNY)		428,128.65	94,076.92
Charging cost (CNY)		2,155,546.75	2,838,479.32
Number of inverters		6	6
Total length of DWC facility (m)		6200	5800
Battery capacity (kWh)	Route 19	99.63	21.31
	Route 56	86.66	17.14
	Route 65	89.99	21.42

85% (Bi et al., 2018) and 90% (He et al., 2020a), respectively. Furthermore, the boundaries for the battery SOC of BEBs throughout the operation are set at 20% (Hwang et al., 2018) and 90% (He et al., 2020a), respectively. The time interval is divided into 1440 segments with a unit time step of 1 min. The length of the segment is assumed to be 400 m. The three routes are consequently divided into 107 segments. Note that Route 19 has a total length of 22.6 km, which cannot be divided into 400 m segments. Hence, the link between node 17 and node 18 is designated as a segment with a length of 200 m.

6.2. Results

The proposed integrated optimization model was implemented in the system. It obtains a model comprising 23,642,371 continuous variables, 247 integer variables, and 23,792,485 constraints. The model was solved using the CPLEX solver (IBM, 2009) and GAMS (Rosenthal, 2012). All numerical studies were conducted on a computer equipped with an Intel (R) Core (TM) i5-8300H CPU running at 2.30 GHz and 16 GB of RAM. The model was solved with a computational time of 384.776s, achieving a relative optimal gap of less than 0.0001%.

The aim of the optimal model presented in this study is to minimize costs related to charging facility, battery, and charging under the TOU tariff mechanism. In order to better demonstrate the significant impact of charging costs on the total cost, a limited model is generated. It aligns with the existing research methods in the implementation of DWC charging facilities. The limited model excludes the charging cost from the original optimal model. It can be formulated by the following program P5:

P5:

$$\begin{aligned} &\min M_4 = Zq^{inv} + \sum_{(i,j)\in A} X_{(i,j)} q^{coil} \Delta l + \sum_{r\in R} \eta_r E_r q^{bat} \\ &s.t. \quad X_{(i,j)}, E_r \in \Theta \\ &\quad \text{Constraints (34), (36)–(42), (44)–(45), and (48)–(53)} \end{aligned} \tag{55}$$

where M_4 is the objective function of the limited model.

Let $M_{total}^{limited}$ denote the total cost of the limited model. It is represented in Eq. (56), as depicted below:

$$\begin{aligned} M_{total}^{limited} = &\sum_{r\in R}\sum_{b\in B_r}\sum_{o=o(r)}\sum_{t\in T_{r,b,o}} \beta q_t P_{r,b,l,o,t} \Delta t + \sum_{r\in R}\sum_{b\in B_r}\sum_{d=d(r)}\sum_{t\in T_{r,b,d}} \beta q_t P_{r,b,d,t} \Delta t \\ &+ \sum_{r\in R}\sum_{b\in B_r}\sum_{(i,j)\in A_r}\sum_{t\in T_{r,b,l,(i,j)}} \alpha q_t X_{(i,j)} P_{r,b,l,t,(i,j)} \Delta t + M_4 \end{aligned} \tag{56}$$

Table 5 provides a comparison between the results obtained from the optimal model and the limited model. The total cost of the battery and charging facility in the optimization model increased by 46.27% compared to the limited model. Additionally, the battery capacity of BEBs on each route increased by 78.61%, 80.22%, and 76.20%, respectively. Despite the increase in battery

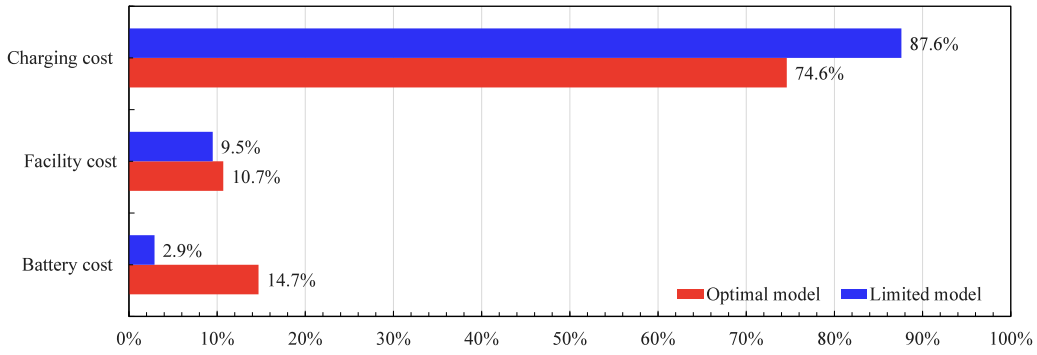

Fig. 9. Comparison of the proportional of costs between the optimal model and the limited model.

capacity and cost, the optimal model considers charging costs in the objective function, leading to a 23.29% reduction in charging costs compared to the limited model. As a result, the total cost in the optimal model decreased by 10.12% compared to the limited model.

Fig. 9 illustrates the proportion of battery cost, charging facility cost, and charging cost in the total cost for both models. It reveals that despite the increased cost of batteries and charging facilities in the optimization model, their combined share in the total cost amounts to only 25.40%. The charging cost, resulting from the charging activities of BEBs, constitutes the most significant portion of the total cost. It also indicates that it is irrational to neglect the optimization of charging scheduling in existing research.

Fig. 10 displays the specific deployment of DWC facilities in the BEB system under the optimal model. It can be observed that the DWC facilities are concentrated at the end and intermediate segments where multiple routes overlap. This is reasonable because installing DWC facilities at these locations enhances the efficient utilization of equipment. To provide a detailed description of the battery SOC of BEBs in the two models, this study plots the battery SOC data for the first BEB on each route, as shown in Fig. 11. The battery SOC of BEBs consistently stays within the range of 20% to 90% during their operation. In the limited model, BEBs need to depend on DWC facilities to replenish their battery energy on every trip due to the smaller battery capacity of BEBs. Even during peak electricity pricing periods, the BEBs have to engage in charging activities to ensure normal operations, resulting in increased charging costs. In contrast, the optimized model improves the battery capacity appropriately. It enables BEBs to sustain regular operations even during periods of peak electricity pricing, eliminating the necessity for recharging. It is effective to avoid charging activities during peak hours. Furthermore, the use of the larger battery capacity in the optimal model also reduces the DOD for BEBs, effectively extending the battery lifespan (Jeong et al., 2015).

Fig. 12 compares the total charging demand throughout a day between the optimization model and the limited model. As shown in Fig. 12(a), it can be observed that BEBs primarily utilize the nighttime with lower electricity prices for charging at the depot in the optimal model. Furthermore, it is worth noting that during the peak electricity price period (11:00 to 13:00), none of the BEBs participate in charging activities. This indicates that considering charging scheduling under the TOU tariff discourages BEBs from charging during peak time, thus resulting in reduced charging costs. Fig. 12(b) further confirms that due to the smaller battery capacity of BEBs in the limited model, a significant amount of charging demand arises during operation. These charging activities are predominantly concentrated at the DWC facilities. In comparison to Fig. 12(a), the charging demand at the DWC facilities for BEBs in the limited model is higher. It is because of their smaller battery capacity that BEBs are unable to avoid charging during peak electricity pricing hours.

Fig. 13 presents a comparison of the results regarding charging costs between the optimization model and the limited model. Combining Figs. 12(a) and 12(b), it is evident that the reduction of charging cost in the optimal model is attributed to a substantial decrease in charging costs during peak hours for BEBs. It amounts to a 54.08% reduction compared to the limited model. From the perspective of charging scheduling of BEBs, the decrease in total charging costs results from a shift of charging activities for BEBs from peak hours to flat and valley hours. Charging during off-peak hours enables BEBs to fulfill their charging demand at a lower cost compared to peak hours. Moreover, BEBs inclined to charge at the depot during the off-peak nighttime period can enhance charging efficiency and reduce energy losses during the charging process. It can also effectively reduce the peak charging demand to alleviate pressure on the urban power grid.

6.3. Sensitivity analysis

To investigate the impact of variations in model parameter values on the final results, a series of experiments were conducted in this study to perform sensitivity analysis on key parameters in the proposed model. These parameters mainly include the nominal charging power of the DWC facility, the DWC facility price, and the energy consumption of BEBs.

Sensitivity analysis results for the nominal charging power of the DWC facility are presented in Fig. 14. It can be observed that as the nominal charging power gradually increases from 60 kW to 100 kW, the total cost decreases. With the increment of the charging power, there are no significant changes in the cost and installation length of the DWC facility. To achieve cost reduction, an increase

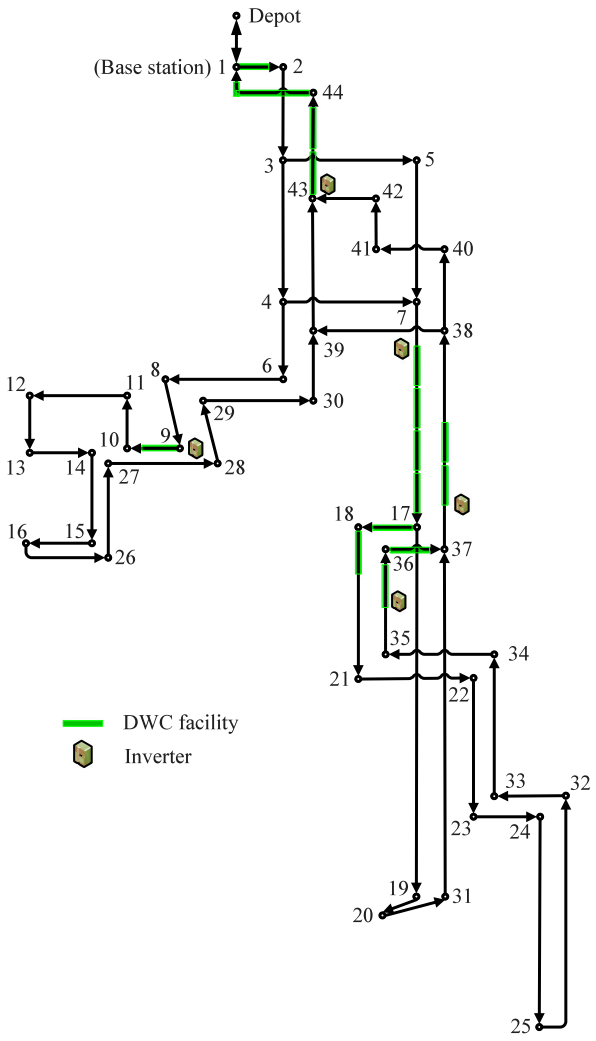

Fig. 10. The optimal deployment of DWC facilities in the BEB system.

in the charging power results in a trade-off between charging cost and battery cost, leading to a rise in the battery capacity of BEBs. It enables BEBs to avoid charging during peak electricity price periods, further shifting the charging demands from peak hours to valley and flat hours. Additionally, the maximum amount of battery energy that BEBs can obtain from the DWC facility within a unit time interval increases with the growth in the nominal charging power. It allows BEBs to replenish more energy during periods of lower electricity prices, thus reducing the total charging cost.

Fig. 15 presents the sensitivity analysis results for the DWC facility price. As the DWC facility price varies from 0.6 to 1.4 times the base case, the total cost continues to increase. To decrease the cost escalation resulting from an increase in DWC facility price, the number of deployed DWC facilities gradually decreases. It leads to a reduction in the available charging time window for BEBs, which affects the battery capacity and charging scheduling for BEBs. It can be observed that as the DWC facility price rises, the battery cost does not increase significantly. This indicates that the BEB system chooses to adjust the charging scheduling strategy rather than increase the battery capacity of BEBs. The BEBs compensate for the limited number of DWC facilities by increasing the energy replenished at existing DWC facilities, ensuring uninterrupted service operations.

Fig. 16 presents the sensitivity analysis results of the energy consumption. As the energy consumption of BEBs varies from 0.6 to 1.4 times the baseline value, there is a noticeable increase in the total cost. This is due to the fact that an increase in energy consumption requires BEBs to carry larger capacity and the charging demands for BEBs also increases. From Fig. 16, it is evident that when aiming to minimize the overall system cost, the battery capacity of BEBs does not increase significantly. Instead, the DWC facility costs and the number of deployments escalate as energy consumption increases. The result indicates that as the energy consumption of BEBs increases, the BEB system tends to construct more DWC facilities. The growing charging cost also suggests that the charging scheduling strategy for BEBs favors utilizing DWC facilities for charging during operation, reducing the battery

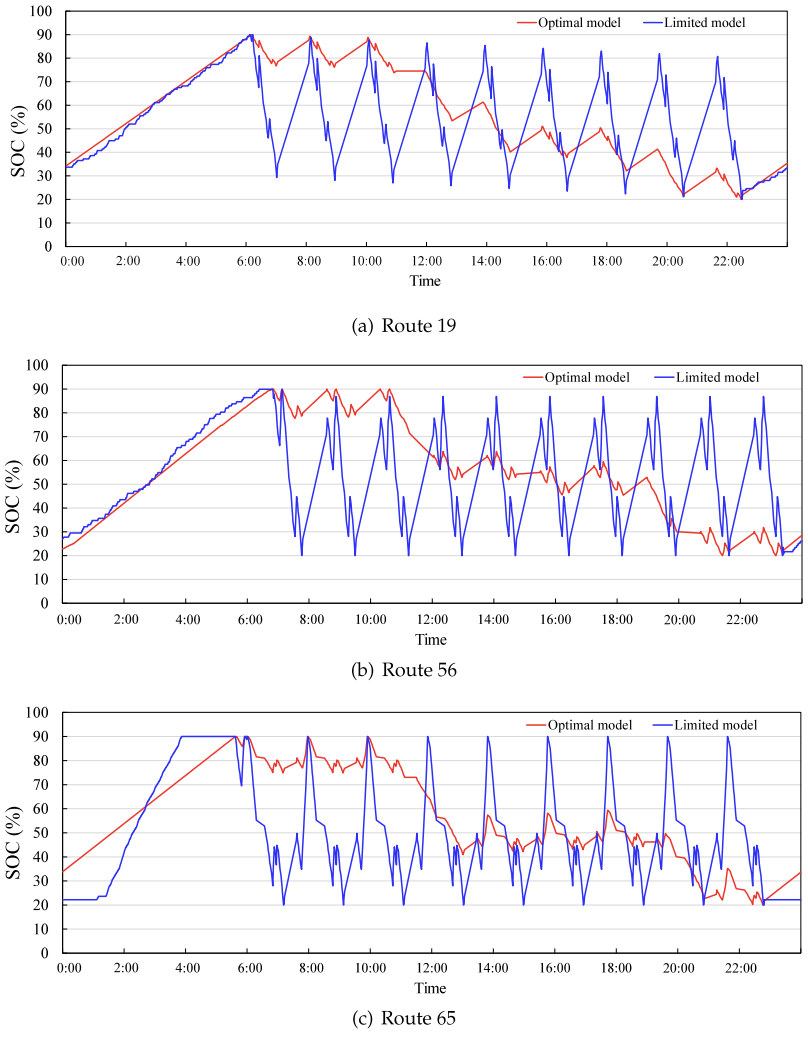

Fig. 11. Battery SOC profiles for the first bus on different routes.

capacity. This conclusion further demonstrates that the application of DWC facilities in BEB systems can effectively reduce the battery capacity of BEBs compared to the plug-in charging method.

7. Conclusion

This study proposes a comprehensive optimization model to address the deployment of DWC facilities and charging scheduling for BEBs under the TOU tariff mechanism for BEB systems.

To describe this problem, a strategic planning model is initially developed to optimize the deployment of DWC facilities and the battery capacity of BEBs. Considering the relation between infrastructure planning and the charging scheduling of BEBs, tactical planning is introduced to optimize the charging scheduling of BEBs under the TOU tariff mechanism. Ultimately, an MINLP model is formulated with the objective of minimizing the total cost, including DWC facility costs, battery costs, and charging costs. To resolve this model, it is reformulated into an MILP model and solved by commercial solvers. Extensive numerical studies are conducted using an actual BEB system in Beijing, China. The results demonstrate that the integrated model reduces the overall cost by 10.12% compared to existing research methods. In terms of charging scheduling optimization, it reduces the charging cost by 23.29%. Therefore, the proposed comprehensive optimization model can efficiently optimize the deployment of charging infrastructure, battery size, and charging scheduling for BEBs. Additionally, it offers practical guidance for operators to implement DWC technology in BEB systems.

However, there are several limitations to the proposed model. It assumes that all BEBs in the system operate based on a predetermined timetable. However, the duration of BEB operation can be affected by traffic congestion. Moreover, the departure schedule of BEBs often adjusts during peak hours to meet passenger travel demands. These factors introduce variations in the

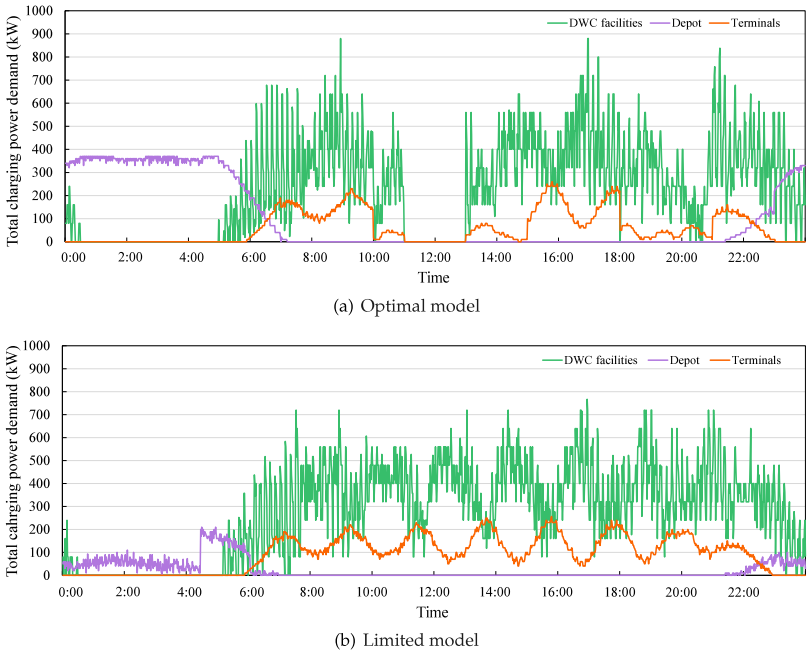

Fig. 12. Total charging power demand profiles for different charging facilities.

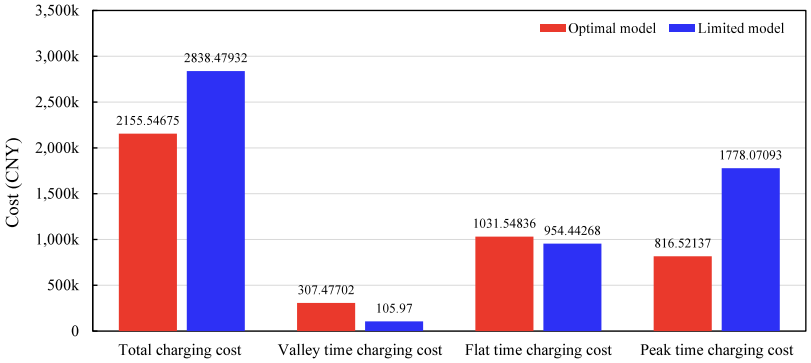

Fig. 13. Comparison of charging costs between the optimal and limited models.

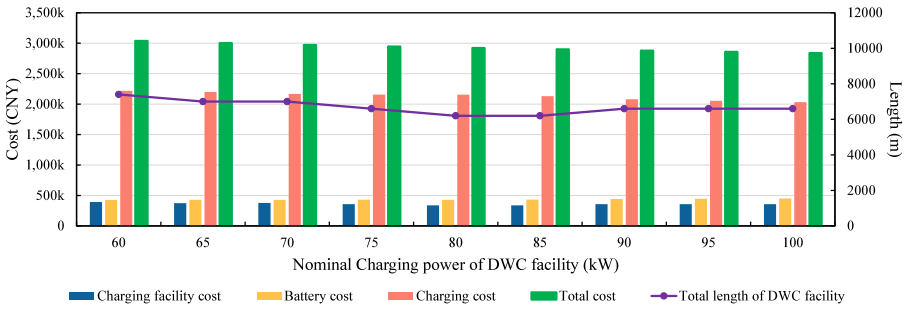

Fig. 14. Sensitivity analysis of the nominal charging power of the DWC facility.

timetable, impacting the charging scheduling for BEBs. Furthermore, the energy consumption of BEBs is affected by many factors, such as BEB speed, passenger load, and road gradient. Owing to the absence of this data, detailed modeling of the energy

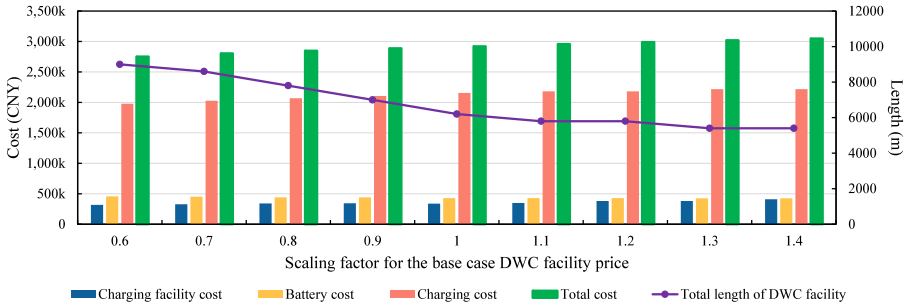

Fig. 15. Sensitivity analysis of the DWC facility price.

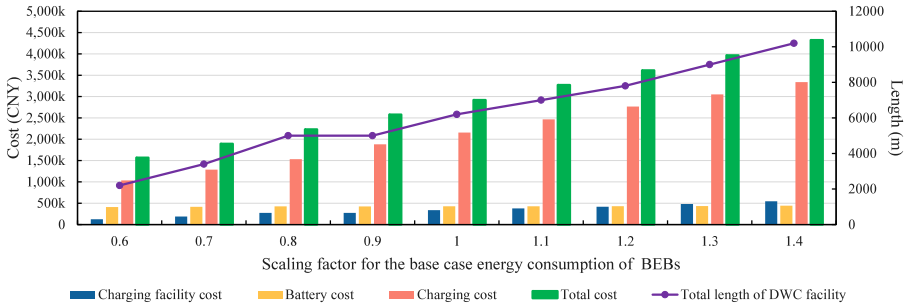

Fig. 16. Sensitivity analysis of the energy consumption of BEBs.

consumption of BEBs has not been undertaken in this study. In future studies, the uncertainties related to the operating time and energy consumption of BEBs will be further incorporated into the proposed optimization model.

CRediT authorship contribution statement

Wenlong Li: Formal analysis, Methodology, Visualization, Writing – original draft. **Yi He:** Conceptualization, Formal analysis, Investigation, Writing – original draft. **Songhua Hu:** Formal analysis, Writing – original draft. **Zhengbing He:** Conceptualization, Supervision, Writing – review & editing. **Carlo Ratti:** Project administration, Writing – review & editing.

Data availability

Data will be made available on request.

Appendix. List of notation

Variables	Description
$X_{(i,j)}$	A binary variable, representing whether the segment (i,j) is equipped by DWC facility or not
$Y_{(i,j)}$	A binary variable, representing whether the segment (i,j) is the initial segment equipped by DWC facility or not
w_i	A binary variable, representing whether the intersection node $i \in N^c$ has incoming segments equipped by DWC facilities or not
$u_{(h,i)}$	A binary variable, representing whether the incoming segment $(h,i) \in A$ of intersection node $i \in N^c$ has covered by inverter or not
Z	The total demand for inverters within the BEB system
$e_{r,b,l,i}$	The residual battery energy of BEB $b \in B_r$ as it reaches the node $i \in N_r$ on route r in service trip $l \in L_{r,b}$
$e^-_{r,b,d}$	The residual battery energy of BEB $b \in B_r$ as it reaches the depot $d(r)$ on route r
$e^-_{r,b,l,o}$	The residual battery energy of BEB $b \in B_r$ as it reaches the terminal $o(r)$ on route r in service trip $l \in L_{r,b}$
$e^+_{r,b,l,o}$	The residual battery energy of BEB $b \in B_r$ as it leaves the terminal $o(r)$ on route r in service trip $l \in L_{r,b}$
$s_{r,b,l,(i,j)}$	The battery energy replenished by BEB $b \in B_r$ as it passes through the segment $(i,j) \in A_r$ on route r in the service trip $l \in L_{r,b}$
$s_{r,b,l,o}$	The battery energy replenished by BEB $b \in B_r$ as it idles in terminal $o(r)$ on route r in the service trip $l \in L_{r,b}$
$s_{r,b,d}$	The battery energy replenished by BEB $b \in B_r$ as it idles in depot $d(r)$ on route r
$\widehat{\Delta c}_r$	The battery consumption per kilometer for BEBs on route r
$c_{r,b,(i,j)}$	The battery energy consumed by BEB $b \in B_r$ on route r as it passes from node $i \in N_r$ to node $j \in N_r$

$c_{r,b,(o,d)}$	The battery energy consumed by BEB $b \in B_r$ as it passes from terminal $o(r)$ to the depot $d(r)$ on route r
$c_{r,b,(d,o)}$	The battery energy consumed by BEB $b \in B_r$ as it passes from depot $d(r)$ to the terminal $o(r)$ on route r
E_r	The battery capacity of BEBs on route r
$P_{r,b,l,(i,j),t}$	The charging power rate of BEB $b \in B_r$ on route r in the segment (i,j) at the time $t \in T$
$P_{r,b,l,o,t}$	The charging power rate of BEB $b \in B_r$ in the terminal $o(r)$ on route r at the time $t \in T$
$P_{r,b,d,t}$	The charging power rate of BEB $b \in B_r$ in the depot $d(r)$ on route r at the time $t \in T$
Parameters	**Description**
$o(r)$	The terminals of on route r
$d(r)$	The depot of on route r
$l^{\Omega}_{r,b}$	The last service trip for BEB $b \in B_r$ on route r
q^{bat}	The amortized cost of the battery per unit
q^{coil}	The amortized cost of transfer coil per unit
q^{inv}	The amortized cost of the inverter per unit
q_t	The electricity price in the time $t \in T$
$e^{+}_{r,b,d}$	The residual battery energy of BEB $b \in B_r$ as it leaves the depot $d(r)$ on route r
ε^{-}	The lower bound of the battery SOC
ε^{+}	The upper bound of the battery SOC
W^{bus}	The curb weight of BEBs
W^{extra}	The passenger weight of BEBs
E^{bus}	The nominal battery capacity of BEBs
Δc	The baseline battery consumption of BEBs
ρ	The energy density of the battery
$l_{(i,j)}$	The length of segment (i,j)
$l_{(o,d)}$	The distance from the base station $o_b(r)$ to the depot $d(r)$
$l_{(d,o)}$	The distance from the depot $d(r)$ to the base station $o_b(r)$
$t_{r,b,l,(i,j)}$	The travel time of BEB $b \in B_r$ on route r as it passes through the segment (i,j) in the service trip $l \in L_{r,b}$
$t_{r,b,l,o}$	The layover time of BEB $b \in B_r$ as it idles in the terminal $o(r)$ on route r in the service trip $l \in L_{r,b}$
$t_{r,b,d}$	The layover time of BEB $b \in B_r$ as it idles in the depot $d(r)$ on route r
$P^{\max 1}$	The nominal charging power of DWC facility
$P^{\max 2}$	The nominal charging power of plug-in charger
α	The charging efficiency rate of DWC facility
β	The charging efficiency rate of plug-in charger
η_r	The fleet size of BEBs on route r
$\tau^{-}_{r,b,l,o}, \tau^{+}_{r,b,l,o}$	The moment when BEB $b \in B_r$ on route r reaches and leaves terminal $o(r)$ in service trip $l \in L_{r,b}$, respectively
$\tau_{r,b,l,i}, \tau_{r,b,l,j}$	The moment when BEB $b \in B_r$ on route r reaches node i and node j in service trip $l \in L_{r,b}$, respectively
$\tau^{-}_{r,b,d}, \tau^{+}_{r,b,d}$	The moment when BEB $b \in B_r$ on route r reaches and leaves depot $d(r)$, respectively
Δt	A unit time interval (min)
Δl	A unit length of a segment (m)
Sets	**Description**
N	Set of nodes in the BEB system, indexed by h, i, and j
N^c	Set of intersection nodes
O	Set of terminals in the system, indexed by o
D	Set of depots in the system, indexed by d
A	Set of segments in the system
B_r	Set of all BEBs on route r, indexed by b
A_r	Set of all segments on route r, $A_r \subseteq A$
N_r	Set of all nodes on route r, $N_r \subseteq N$
$L_{r,b}$	Set of service trips for BEBs $b \in B_r$ on route r, indexed by l
R	Set of routes in the system, index by r
T	Set of time intervals in one day, $T = \{1, 2, \ldots, \frac{1440}{\Delta t}\}$, indexed by t
$T_{r,b,d}$	Set of the available charging time windows when BEB $b \in B_r$ idles in the depot $d(r)$ on route r
$T_{r,b,l,(i,j)}$	Set of the available charging time windows when BEB $b \in B_r$ travels at segment $(i,j) \in A_r$ on route r in service trip $l \in L_{r,b}$
$T_{r,b,l,o}$	Set of the available charging time windows when BEB $b \in B_r$ idles in the terminal $o(r)$ on route r in service trip $l \in L_{r,b}$

References

Abdelwahed, A., van den Berg, P.L., Brandt, T., Collins, J., Ketter, W., 2020. Evaluating and optimizing opportunity fast-charging schedules in transit battery electric bus networks. Transp. Sci. 54 (6), 1601–1615.

Alwesabi, Y., Avishan, F., Yanıkoğlu, İ., Liu, Z., Wang, Y., 2022. Robust strategic planning of dynamic wireless charging infrastructure for electric buses. Appl. Energy 307, 118243.

Alwesabi, Y., Liu, Z., Kwon, S., Wang, Y., 2021. A novel integration of scheduling and dynamic wireless charging planning models of battery electric buses. Energy 230, 120806.

An, K., 2020. Battery electric bus infrastructure planning under demand uncertainty. Transp. Res. C 111, 572–587.

Bai, Z., Yang, L., Fu, C., Liu, Z., He, Z., Zhu, N., 2022. A robust approach to integrated wireless charging infrastructure design and bus fleet size optimization. Comput. Ind. Eng. 168, 108046.

Bi, Z., Keoleian, G.A., Ersal, T., 2018. Wireless charger deployment for an electric bus network: A multi-objective life cycle optimization. Appl. Energy 225, 1090–1101.

Bi, Z., Keoleian, G.A., Lin, Z., Moore, M.R., Chen, K., Song, L., Zhao, Z., 2019. Life cycle assessment and tempo-spatial optimization of deploying dynamic wireless charging technology for electric cars. Transp. Res. C 100, 53–67.

Bi, Z., Song, L., De Kleine, R., Mi, C.C., Keoleian, G.A., 2015. Plug-in vs. Wireless charging: life cycle energy and greenhouse gas emissions for an electric bus system. Appl. Energy 146, 11–19.

Bolger, J., Kirsten, F., Ng, L., 1978. Inductive power coupling for an electric highway system. In: 28th IEEE Vehicular Technology Conference, Vol. 28. pp. 137–144.

Boyer, V., Ibarra-Rojas, O.J., Ríos-Solís, Y.Á., 2018. Vehicle and crew scheduling for flexible bus transportation systems. Transp. Res. B 112, 216–229.
Chen, Z., He, F., Yin, Y., 2016. Optimal deployment of charging lanes for electric vehicles in transportation networks. Transp. Res. B 91, 344–365.
Chen, Z., Yin, Y., Song, Z., 2018. A cost-competitiveness analysis of charging infrastructure for electric bus operations. Transp. Res. C 93, 351–366.
Cirimele, V., Diana, M., Freschi, F., Mitolo, M., 2018. Inductive power transfer for automotive applications: state-of-the-art and future trends. IEEE Trans. Ind. Appl. 54 (5), 4069–4079.
Foton, 2022. Details of the foton AUV EU5 (BJ6109) pure electric urban bus. https://auv.foton.com.cn/webback/car/model/114.
Fuller, M., 2016. Wireless charging in california: range, recharge, and vehicle electrification. Transp. Res. C 67, 343–356.
He, Y., Liu, Z., Song, Z., 2020a. Optimal charging scheduling and management for a fast-charging battery electric bus system. Transp. Res. E 142, 102056.
He, Y., Liu, Z., Song, Z., 2022a. Integrated charging infrastructure planning and charging scheduling for battery electric bus systems. Transp. Res. Part D 111, 103437.
He, J., Yan, N., Zhang, J., Yu, Y., Wang, T., 2022b. Battery electric buses charging schedule optimization considering time-of-use electricity price. J. Intell. Connected Veh. 5 (2), 138–145.
He, J., Yang, H., Tang, T.-Q., Huang, H.-J., 2020b. Optimal deployment of wireless charging lanes considering their adverse effect on road capacity. Transp. Res. C 111, 171–184.
Hu, H., Du, B., Liu, W., Perez, P., 2022. A joint optimisation model for charger locating and electric bus charging scheduling considering opportunity fast charging and uncertainties. Transp. Res. C 141, 103732.
Hwang, I., Jang, Y.J., Ko, Y.D., Lee, M.S., 2018. System optimization for dynamic wireless charging electric vehicles operating in a multiple-route environment. IEEE Trans. Intell. Transp. Syst. 19 (6), 1709–1726.
IBM, 2009. CPLEX V12. 1: User's Manual for CPLEX. International Business Machines Corporation.
IEA, 2021. Transport improving the sustainability of passenger and freight transport. https://www.iea.org/topics/transport.
Jansuwan, S., Liu, Z., Song, Z., Chen, A., 2021. An evaluation framework of automated electric transportation system. Transp. Res. Part E 148, 102265.
Jeong, S., Jang, Y.J., Kum, D., 2015. Economic analysis of the dynamic charging electric vehicle. IEEE Trans. Power Electron. 30 (11), 6368–6377.
Lee, J., Shon, H., Papakonstantinou, I., Son, S., 2021. Optimal fleet, battery, and charging infrastructure planning for reliable electric bus operations. Transp. Res. D 100, 103066.
Lin, Y., Zhang, K., Shen, Z.-J.M., Ye, B., Miao, L., 2019. Multistage large-scale charging station planning for electric buses considering transportation network and power grid. Transp. Res. C 107, 423–443.
Liu, T., Ceder, A., 2020. Battery-electric transit vehicle scheduling with optimal number of stationary chargers. Transp. Res. C 114, 118–139.
Liu, K., Gao, H., Wang, Y., Feng, T., Li, C., 2022. Robust charging strategies for electric bus fleets under energy consumption uncertainty. Transp. Res. D 104, 103215.
Liu, Z., Song, Z., 2017. Robust planning of dynamic wireless charging infrastructure for battery electric buses. Transp. Res. C 83, 77–103.
Liu, H., Zou, Y., Chen, Y., Long, J., 2021. Optimal locations and electricity prices for dynamic wireless charging links of electric vehicles for sustainable transportation. Transp. Res. E 152, 102187.
Ma, X., Miao, R., Wu, X., Liu, X., 2021. Examining influential factors on the energy consumption of electric and diesel buses: A data-driven analysis of large-scale public transit network in Beijing. Energy 216, 119196.
MEE, 2021. China mobile source environmental management annual report. https://www.mee.gov.cn/hjzl/sthjzk/ydyhjgl/202109/t20210910_920787.shtml.
Ngo, H., Kumar, A., Mishra, S., 2020. Optimal positioning of dynamic wireless charging infrastructure in a road network for battery electric vehicles. Transp. Res. D 85, 102385.
Perumal, S.S.G., Lusby, R.M., Larsen, J., 2022. Electric bus planning & scheduling: A review of related problems and methodologies. European J. Oper. Res. 301 (2), 395–413.
Rogge, M., van der Hurk, E., Larsen, A., Sauer, D.U., 2018. Electric bus fleet size and mix problem with optimization of charging infrastructure. Appl. Energy 211, 282–295.
Rosenthal, R.E., 2012. GAMS—a User's Guide.. GAMS Development Corporation, Washington, D.C..
Rupp, M., Rieke, C., Handschuh, N., Kuperjans, I., 2020. Economic and ecological optimization of electric bus charging considering variable electricity prices and CO2eq intensities. Transp. Res. D 81, 102293.
Tan, Z., Liu, F., Chan, H.K., Gao, H.O., 2022. Transportation systems management considering dynamic wireless charging electric vehicles: review and prospects. Transp. Res. E 163, 102761.
Tang, X., Lin, X., He, F., 2019. Robust scheduling strategies of electric buses under stochastic traffic conditions. Transp. Res. C 105, 163–182.
Wang, Y., Liao, F., Lu, C., 2022. Integrated optimization of charger deployment and fleet scheduling for battery electric buses. Transp. Res. D 109, 103382.
Wang, X., Song, Z., Xu, H., Wang, H., 2023. En-route fast charging infrastructure planning and scheduling for battery electric bus systems. Transp. Res. D 117, 103659.
Xie, D.-F., Yu, Y.-P., Zhou, G.-J., Zhao, X.-M., Chen, Y.-J., 2023. Collaborative optimization of electric bus line scheduling with multiple charging modes. Transp. Res. D 114, 103551.
Xylia, M., Leduc, S., Patrizio, P., Kraxner, F., Silveira, S., 2017. Locating charging infrastructure for electric buses in stockholm. Transp. Res. C 78, 183–200.
Zhang, L., Zeng, Z., Gao, K., 2022. A bi-level optimization framework for charging station design problem considering heterogeneous charging modes. J. Intell. Connect Veh. 5 (1), 8–16.